Continuous Adsorption of Humins by Using Granulated Activated Carbon

By

Lovisa Engström
Isabelle Larsson

Department of Process and Life Science Engineering
Lund University

May 2024

Supervisor: **Postdoc Mikael Sjölin**
Co-supervisor: **Postdoc Mahmoud Sayed Ali Sayed**
Examiner: **Professor Ola Wallberg**

Postal address
P.O. Box 124
SE-221 00 Lund, Sweden
Web address
www.ple.lth.se

Visiting address
Getingevägen 60

Telephone
+46 46-222 82 85
+46 46-222 00 00

Acknowledgements

This master thesis was conducted during the spring of 2024 at the institution of Process and Life Science Engineering at LTH, Lund. First, we would like to greatly thank our supervisor Mikael Sjölin, who has guided us though this whole process. Thank you for always keeping your office door open. We would also like to thank our co-supervisor Mahmoud Sayed Ali Sayed for your support and a much needed helping hand when we were struggling. Also, a special thank you to Daniel Espinoza for sharing your Python model of the adsorption column, which made modelling the isotherm and kinetic models possible.

Furthermore, many thanks to all our friends and colleagues at the department for the helpful and inclusive atmosphere, and the company around the fika and lunch table. Your positive energy has been important on our rough days. Lastly, we want to thank Ola Wallberg for taking the responsibility to be our examiner in this thesis.

Abstract

The demand for plastics is growing due to global population, economic growth and insufficient recycling, where new bio-based feedstocks must be investigated to meet future emission goals. 5-Hydroxymethylfurfural (HMF) is a promising platform chemical that can produce Polyethylene furanoate (PEF) with similar characteristics to fossil-based polyethylene terephthalate (PET). The HMF can be produced by dehydration of fructose, where sugar beet molasses is a promising low-value feedstock in Sweden. However, the dehydration also results in formation of byproducts called humins, which require downstream purification. This thesis investigated experimentally if continuous adsorption with granulated activated carbon efficiently could remove these byproducts, examining the effect of temperature and residence time.

The production of HMF never reached a stable operating point varying reactor design, pH, residence time and catalyst. The adsorption experimental results showed that the adsorption of humins was favored by an increased temperature, indicating that the diffusion had a larger impact than the increase in solubility when increasing the temperature. The adsorption of HMF was unaffected by changes in temperature. The adsorption reached 95% removal of impurities and a recovery of 52% of HMF at 55°C and a residence time of 16 minutes. Further, a trade-off between HMF loss, productivity and energy demand needs to be considered for scale-up. The adsorption of the impurities can be described by the BET isotherm and pseudo first order kinetics. All the models evaluated for HMF fitted the experimental data set well. However, the Langmuir isotherm and pseudo first order kinetics are the simplest. The modelling was only based on one dataset, and there is a risk of overfitting where more data is needed to further evaluate and confirm the accuracy of the proposed models.

Populärvetenskaplig sammanfattning

Världen idag är i ett stort behov av att byta ut fossila råvaror mot mer hållbara alternativ. Nya processer behöver utvecklas för att minska våra utsläpp, bland annat tillverkning av icke fossilbaserade plaster. Plasten polyetylenfuranoat (PEF) har visat stor potential som alternativ till PET, och kan tillverkas av 5-hydroymetylfurfural (HMF). HMF kan bland annat framställas från fruktos, vilket kan utvinnas från restprodukter av sockerindustrin. Att använda restprodukter innebär ytterligare en hållbarhetsaspekt, då detta inte ger ytterligare miljöpåverkan genom att använda resurser som finns tillgängliga. Utöver att processen är hållbar behöver den också vara produktiv och kostnadseffektiv för att ha potential att konkurrera med nuvarande fossila råvaror.

När man använder fruktos för att framställa HMF via en reaktion bildas även en mängd olika biprodukter. I framställningen är det önskvärt att reagera så stor mängd som möjligt av fruktosen, som sedan främst ska bilda HMF och så lite biprodukter som möjligt. Reaktionssteget behöver därför utforskas för att använda sig av driftsparametrar och en reaktordesign som ger optimerade resultat.

I nästa steg av processen måste dessa biprodukter separeras för att få en ren produkt. Detta kan göras genom adsorption, en metod som utnyttjar de olika ämnenas benägenhet att fästa sig på ett fast material. Den orena produkten förs genom ett rör packat med fast granulerat aktivt kol. I detta fall vill man adsorbera orenheterna på ytan av kolet, samtidigt som den önskade föreningen HMF stannar kvar i lösningen som flödar förbi kolet och ut som upprenad produkt.

I detta examensarbete utreds framställningen av HMF från fruktos genom att först hitta en optimal reaktordesign för att sedan utreda driftsparametrar. Lösningen renas sedan genom adsorption där olika kontakttider med kolet och temperaturer testas, för att sedan använda insamlade data för att utforska modeller som kan beskriva upprepningen. Dessa modeller kan i sin tur användas för att förstå processen ytterligare, och möjliggör en djupare förståelse vid en uppskalning av processen.

Experimenten visade en svårighet i att uppnå en stabil drift vid reaktion, som resulterade i sämre resultat än väntat. Detta steg behöver utredas ytterligare för att i framtiden vara en lönsam process. Uppreningen gav väntade resultat och kunde rena bort 94% av orenheterna, men som tyvärr också visade att 48% av mängden HMF också band in till kolet. Här finns möjligheter att testa metoder som förhoppningsvis kan få HMF att släppa från kolet, utan att samtidigt få med sig orenheterna. På grund av den ostabila driften i reaktionssteget fanns inte möjlighet att samla in tillräckligt med data för att beskriva uppreningen helt och hållet, men det visade på att det finns tydliga trender och stor potential att utveckla vidare med mer data.

Table of Content

1. Introduction 1

1.1. Aim 1

2. Background 3

2.1. 5-Hydroxymethylfurfural 3

2.2. Fructose Dehydration 4

2.2.1. Humins 4

2.2.2. Homogenous and Heterogenous Catalysts for the dehydration reaction 5

2.2.3. Biphasic Reaction System 5

2.2.4. Organic Solvent Selection 6

2.3. Adsorption 7

2.3.1. Granular Activated Carbon 8

2.3.2. Isotherms 8

2.3.3. Kinetic Models 10

2.3.4. Continuous Packed bed Adsorption of Humins 11

2.3.5. Desorption 12

2.4. Analysis 12

2.4.1. HPLC 12

2.4.2. UV-Vis Spectroscopy 13

3. Method 14

3.1. Continuous Dehydration of Fructose 14

3.2. Fixed Bed Adsorption 15

3.3. Analytic Methods 16

3.3.1. HPLC 16

3.3.2. UV-Vis Spectroscopy 16

3.4. Modelling Adsorption Kinetics 16

4. Results & Discussion 18

4.1. Dehydration Reaction Experiments 18

4.1.1. Tube Reactor Design 18

4.1.2. Flowrate Experiments 19

4.1.3. Big Batch 22

4.2. Adsorption Experiments 22

4.2.1. Effect of Residence Time 22

4.2.2. Effect of Temperature 25

4.3. Adsorption Kinetic Models 27

4.4. Future Improvements 30

5. Conclusion 31

6. References 32

Appendix **36**

1. Introduction

Today, the chemical industry is heavily dependent on fossil resources and it is responsible for about 5 percent of the total carbon dioxide emissions [1]. The industry needs to develop sustainable alternative processes to limit the emissions to reach the Swedish zero net greenhouse gas emissions by 2045 [2].

The chemical industry plays a huge role in many sectors including agriculture, food, transportation, and packaging. The development of viable and sustainable processes producing chemicals and fuels from biomass has gained a lot of attention in recent years due to environmental issues related to depleting fossil resources. The demand for plastics is growing due to global population and economic growth, and insufficient recycling. On top of that, plastics can only be recycled a limited number of times [3]. The global plastic production is expected to reach 590 million tons of virgin material by 2050 [4]. This development is expected to result in the plastic industry representing 20 percent of the global oil consumption by 2050 [3]. Therefore, new bio-based feedstocks for plastic production need to be identified to meet the future demands and emission goals.

Polyethylene furanoate (PEF) is one promising candidate on development in this area. It can be used as an alternative to fossil-based polyethylene terephthalate (PET), which represents 22.5% of the global plastic production today. The life cycle global warming potential (GWP) for PEF has shown to be 50-74% lower than for conventional PET.[5] 2,5-Furandicarboxylic acid (FDCA) is the key monomer in production of PEF which can be produced by 5-Hydroxymethylfurfural (HMF).[6] Besides from being an intermediate in production of PEF, HMF is versatile platform chemical that can be used in production of pharmaceuticals, biofuels and other furan-based polymers.[7]

HMF can be produced through dehydration of fructose. In an ongoing project by Sjölin (2023)[7] at Lund University, it has been found that sugar beet molasses is a promising feedstock in Sweden. It both has a high sugar content and is a low value by-product from the processing of sugar beets. This is a promising process for the future, both by producing a biobased platform chemical as well as utilizing waste products from other already existing processes. The dehydration produces a large amount of by-products, called humins, which require further downstream processing. This needs to be investigated further to allow scale-up of the process.

1.1. Aim

This master thesis has been performed at the department of Process and Life Science Engineering, Lund University. The aim of the thesis was to experimentally evaluate if continuous adsorption of humins using granulated activated carbon can efficiently remove impurities in the downstream purification in 5-Hydroxymethylfurfural (HMF) production. The

thesis also includes tube reactor design and production of HMF by dehydration of fructose, as well as evaluation of isotherm and kinetic models for the adsorption.

2. Background

The background for this thesis is based on the ongoing project by Sjölin (2023)[7], where a process for producing HMF from sugar beet molasses has been researched. Molasses consists mainly of sucrose, which can be broken down to one glucose and one fructose unit. The process consists of different steps, which can be seen in Figure 1.

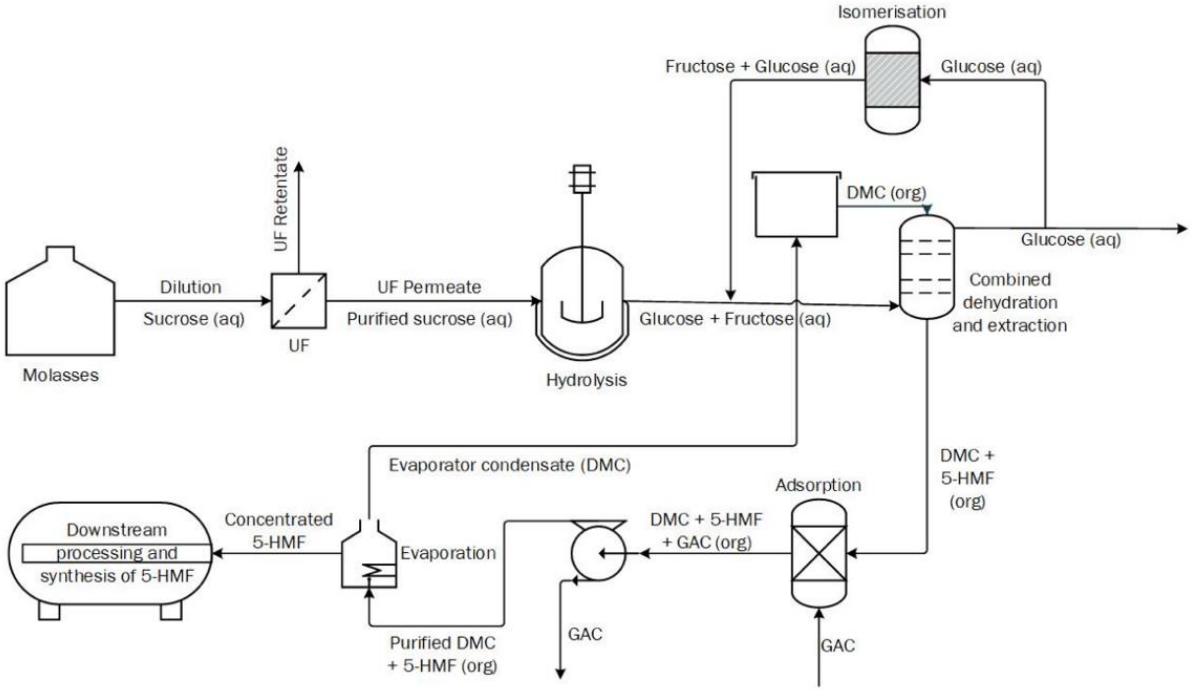

Figure 1. The process flow diagram for the production of HMF, constructed by Sjölin (2023)[7].

The downstream processing is an important part of the process because of the byproduct formation of humins, where the adsorption plays a key role. The adsorption has only been investigated experimentally in batch by adding granulated activated carbon to the DMC and HMF mixture. For further scale-up of the process, the adsorption is more effectively carried out in a continuous mode.[7]

2.1. 5-Hydroxymethylfurfural

HMF has a good variety of functionality because of the structure, including a furan ring with one hydroxyl and one aldehyde group, see Figure 2. It is considered a promising platform chemical in future bio-refineries [8]. It has a boiling point between 114 and 116 degrees Celsius and is soluble in a range of solvents like water, methanol, acetone, formaldehyde, benzene etc. [9]. HMF can be used to derive a variety of value adding chemicals including bioplastics, biofuels and drugs making it highly attractive [10]. The industrial importance of HMF has resulted in growing research of the development of technologies to produce the chemical.

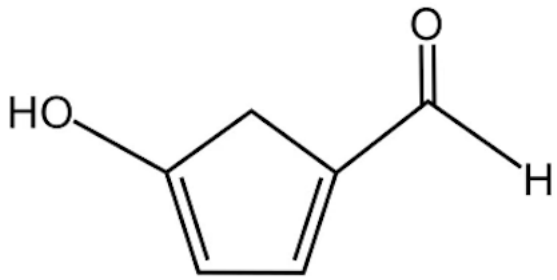

Figure 2. The molecular structure of 5-Hydroxymethylfurfural (adapted from Melo et.al. (2014)[11]).

2.2. Fructose Dehydration

Hexoses, including glucose, fructose and xylose, are the most abundant monosaccharides in biomass and can be used to produce a variety of chemicals. HMF can be produced by acid-catalyzed dehydration of fructose, see Figure 3. The reaction removes three water molecules from the fructose molecule.[12] However, there is a large number of side-reactions that occur including re-hydration to formic acid (FA), levulinic acid (LA) and cross polymerization to soluble polymers and insoluble humins.[9] HMF could also be produced from glucose, but studies have shown that fructose gives a more selective formation of HMF than glucose.[9] Therefore the production of HMF in this study will be based on dehydration of fructose.

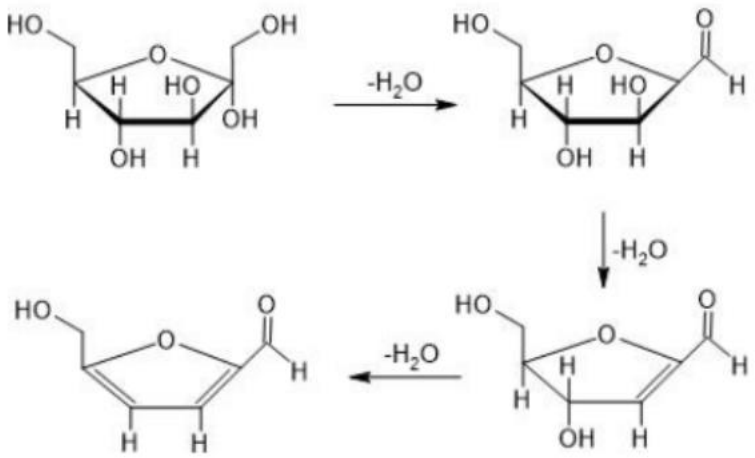

Figure 3. The dehydration reaction of fructose to form HMF.[7]

2.2.1. Humins

The formation of humins is observed like solid dark colored byproducts (impurities) in the product solution. The structure is composed of mainly furan rings, carbonyl, and carboxyl groups, depending on the intermediates and the size of the molecules varies. The formation is unwanted since it results in a lower yield for the dehydration reaction. Additionally, it can clog the continuous system by covering tubes and reactor walls. Therefore, researchers have investigated how to prevent humin formation by optimizing the reaction conditions such as pH,

temperature, and reaction time. High temperature and long reaction time accelerate the formation of humin particles and the level of agglomeration. When cross-linking into a larger network structure the humins become insoluble.[13] In pH range of 0-1 the particles formed has a more varying and irregular shape, and when increasing the initial pH the particles decreased in size but perhaps also the overall process yield.[13] The humin formation results in 10-50% carbon loss from the feed, negatively affecting the process economy. Today, humins are used in low value applications, for example in biorefineries to supply heat by combustion.[14]

2.2.2. Homogenous and Heterogenous Catalysts for the dehydration reaction

Catalytic dehydration of fructose to HMF has been extensively investigated, using both heterogenous and homogenous catalysts. Heterogenous catalysts are often preferred since they can easily be separated and reused. Although, frequent regeneration is required due to byproducts depositing on the catalyst surface and blocking the active sites. In addition, these are toxic and expensive for large scale production.[15] The heterogenous catalysts should be avoided in continuous operation since there is a risk of blocking [16]. There are nearly one hundred acidic inorganic and organic homogenous catalyst that has been identified to catalyze the dehydration reaction. The most common ones used are sulphuric acid, phosphoric acid and hydrochloric acid since they are available at a low cost.[9]

Moreover, researchers have also used ionic liquids such as 1-butyl-3-methylimidazolium, 1-octyl-methylimadizolium etc. Liquid ions are salts of ions that are liquid at room temperatures or below 100 degrees Celsius. The advantage is that the chemical and physical properties can be tuned by varying the ions and it can act as solvent and have catalytic properties at the same time.[9] The ionic liquids can convert raw biomass into final product directly. However, there are numerous drawbacks like reduced mass transfer, severe corrosion in presence of water, sensitivity to impurities and moisture, high cost etc. Lastly HMF is sensitive to heat, requiring special distillation techniques to efficiently separate HMF from the ionic liquid.[9]

2.2.3. Biphasic Reaction System

Another concern in the HMF production is the solvent use. Studies have used water as a solvent since it is non-toxic and abundant. However, the selectivity was very low for HMF and the product was hard to extract. This is due to HMF being highly water soluble.[15] By adding HCl in water, the selectivity of the reaction increased, and by using a mixture of 2-butanol and methyl isobutyl ketone (MIBK) the extraction efficiency increased. Further, these HCl-catalyzed aqueous-organic biphasic systems was determined to be attractive for larger production due to low catalyst cost, easy separation, and high yields of HMF.[15] Using biphasic reaction system integrates the liquid-liquid extraction, using an organic phase with the production step.[15] The biphasic reaction medium is preferably water-immiscible low boiling point organic solvents to isolate HMF to prevent it to react further in the water phase and to allow for easy downstream separation.[17] The partition coefficient (concentration in organic phase versus concentration in water phase) must also be high enough for good product recovery

in the organic phase. Otherwise, if the value is low the system will require a large volume of the organic phase that needs to be processed downstream.[9]

It has been observed that a significant fraction of HMF remains in the aqueous phase, showing poor partitioning between the organic and water phases [18]. To increase the phase separation and partitioning of the HMF into the organic phase, salt can be added resulting in a higher yield. In a study, THF was used as the organic solvent and the effect of LiCl, NaCl and KCl on the extraction was studied. The results showed that NaCl at high concentrations resulted in the largest partitioning of HMF into THF. However, this step will require further downstream processing.[19]

Experiments of a biphasic system has been made in a batch reactor to study the effect of reaction temperature and concentration of acid catalyst. The results showed that higher temperature or acid concentration increased the dehydration reaction rate. The increased temperature also resulted in a higher yield of HMF at a shorter reaction time. This implied that the activation energy was higher for the dehydration to HMF than for the side reactions forming by-products.[20] The dehydration reaction requires a pH below 2 [7].

2.2.4. Organic Solvent Selection

Many researchers have studied the biphasic system substate conversion, selectivity, and yield for several low boiling organic solvents. When selecting a solvent for industrial use, environmental policies and restrictive regulations needs to be considered.[21] In an earlier part of the project, Sayed et al. (2020)[16] has screened MIBK, dimethyl carbonate (DMC),1-butanol, tetrahydrofuran (THF), 2-propanol and γ-Valerolactone (GVL) for the acid-catalyzed dehydration reaction. Using the GlaxoSmidthKline (GSK) solvent sustainability guide, the study found that 1-butanol, DMC and MIBK have the highest overall sustainability. GVL was excluded since it has a high boiling point and similar structure as HMF, which would make separation difficult. The fructose conversion, yield, and productivity were measured on samples from experiments conducted in vials using HCl as acidic catalyst. The results showed that 1-butanol and MIBK gave the lowest fructose conversion. The MIBK system also formed visible amounts of humins, which was explained by the low partitioning coefficient of HMF in MIBK. The DMC system obtained a conversion of 50.4 ±9.3% and a higher selectivity and productivity. Based on the results DMC was chosen the most suitable solvent for the dehydration reaction. In addition, fructose cannot dissolve in DMC, which separates the non converted fructose from the product efficiently. It was also concluded that DMC bound to HMF with strong hydrogen bonds, hindering side reactions.[16]

Further, the same study also did experiments in a continuous reactor with a volume of 9.4 ml at a flowrates of 7.9, 9 and 10 ml/min (residence times between 0.94-1.19 min). The following experimental parameters was used: fructose concentration of 300 g/l, DMC:water ratio of 3:1 and 180°C. The experiment with a flowrate of 10 ml/min resulted in the highest conversion, yield and selectivity of 98.7, 84.8 and 85.9 percent respectively.[16] Therefore, DMC was

selected for experimental part of the project when researching continuous operation for up-scaling to industrial scale.

2.3. Adsorption

Adsorption is a separation method where molecules (adsorbate) attach to the surface of a solid (adsorbent). The adsorption process can be classified either as Physical (physisorption) or Chemical (chemisorption). In physical adsorption the adsorbate bonds physically with the adsorbent through weak Van der Waal's bonds or affinity, and in chemical adsorption they bond chemically.[22] To describe how much adsorbate can be adsorbed, the load, q, can be used. The load can be expressed as mass adsorbate per mass adsorbent, and several factors can have an impact on the magnitude of the load. The porosity, particle size and surface area of the adsorbent are of great importance, as well as the interaction between the surface of the solid and the adsorbate.[23] Other factors such as contact time, pH, temperature, and concentration can also affect the adsorption. In a continuous process, the contact time can be controlled by the residence time in the packed adsorption column.[23]

A continuous adsorption process can be conducted by using a fixed bed, where the adsorbent is packed in a column and the solution containing the adsorbate is pumped through the bed. In the column, the ratio between adsorbent and solution is high and it is assumed that equilibrium is reached immediately as the solution comes in contact with the packed bed. To allow for scale up of an adsorption process, and to be able to model the isotherm and adsorption rate, a breakthrough curve is needed. The breakthrough curve is composed by plotting the outlet concentration against time.[24] In order to get the residence time, an interstitial velocity through the column is needed, see equation 1.[25]

$$v_{int} = \frac{F\tau}{\varepsilon A} \tag{1}$$

The interstitial velocity, v_{int} (m/s)$_t$, is described by the volumetric flowrate F (m^3/s) into the column, together with the cross sectional area A (m^2), the porosity of the bed ε and the tortuosity τ. The porosity ε can be described by the volume of the void, V_{void} (m^2), and the total volume, V_{tot} (m^2), see equation 2. The tortuosity can be described by the actual length, L_e (m), of flow channels and the length of the porous medium, L (m), see equation 3.[25]

$$\varepsilon = \frac{V_{void}}{V_{tot}} \tag{2}$$

$$\tau = \frac{L_e}{L} \tag{3}$$

The diffusion of the adsorbate to the adsorbent is directly correlated to the temperature, where an increased temperature gives faster diffusion.[26] On the other hand, the adsorption is favored by low temperatures since solubility increases with temperature and the potential to bind will decrease. This means that the adsorbate rather stay in the solution than bind to the adsorbent.[27] Therefore it is interesting to evaluate the effect of temperature.

2.3.1. Granular Activated Carbon

Adsorption by using activated carbon as adsorbent is of great importance for the water industry, to remove contaminants, natural organic material, and other naturally occurring compounds that are unwanted in drinking water. Activated carbon adsorbs by hydrophobic interactions and consists of a very porous material, resulting in a large internal surface area. The surface area of the adsorbent is a key part of adsorption since it provides the sites for molecules to adsorb on. There are different types of activated carbon, and they have a variety of pore sizes. Granular activated carbon (GAC) can be used in the water treatment and due to its high mass it gives a very large surface area. The GAC must be replaced or regenerated over time, leading to increased production costs for maintenance.[28] However, compared to other adsorbents, GAC has a relatively low price.[29]

Brunauer–Emmett–Teller (BET) theory is a simplified method used for describing adsorption of gases, which today is commonly used to determine surface area of different adsorbents, but also of catalysts. Three types of pores with different widths have been observed, macropores (<50 nm), mesopores (2-50 nm) and micropores (<2 nm). [30] In general, a high BET surface area results in a more efficient adsorption, since it normally means smaller pores.[31] Sjölin (2023)[7] screened eight different GAC types in batch adsorption experiments of humins. The selection depended on the loading and carbon surface structure. The results showed that Organosorb 20-AA resulted in the highest impurity removal of 97.6 ± 1.3% and a HMF loss of 36.4 ± 24%. The BET surface of Organosorb 20-AA was 830 m^2g^{-1}, which was surprisingly the smallest of the screened GACs. The dose of GAC was optimized to reduce the amount of HMF lost in the adsorption. The results showed that 2-4 g/20 mL resulted in the lowest HMF reduction of approximately 20% and impurity reduction of 80%.[7]

The system pH can change the surface charge of the GAC and effect the equilibrium of the adsorption system.[32] The active carbon interacts with hydrophobic interactions and the furan ring of the HMF will bind. Therefore, it is not likely that the interactions will be affected by pH variations, but it has not been studied in the batch experiments. However, the reaction is catalyzed by an acid. Decreasing the pH could therefore increase the reactivity of HMF and risk the formation of more byproducts.[33] The effect of temperature on HMF adsorption on GAC has been investigated in batch. The results showed that more HMF was adsorbed at lower temperatures.[33]

2.3.2. Isotherms

When the contact time between the adsorbate and the adsorbent is long enough, an equilibrium between the number of adsorbed molecules and the desorbed molecules from the adsorbate to the adsorbent develops. The equilibrium at a certain temperature can be described by a model called isotherm. Today there are over 100 different models that predict the equilibrium distribution for different systems. All systems are based on thermodynamics and mathematical principles of physical adsorption.[23] In order obtain an efficient adsorption, the goal is to get a favorable isotherm. A favorable isotherm has a high load , q, at low inlet concentrations of adsorbate, that levels off as the inlet concentration increases.[25]

Two common models to describe the isotherm are Langmuir and Freundlich isotherms. The Langmuir isotherm is described in equation 4, and is based on a maximum number of available sites on the adsorbent.[23] The higher the K in the equation, the more favorable isotherm is achieved. For the Freundlich isotherm in equation 5, there is no saturation, which can be the case when adsorption occurs in several layers. If n=1 the isotherm is linear, which is unfavorable. A favorable Freundlich isotherms is achieved when n<1.[25]

$$q_{eq} = q_{max} \frac{KC_{eq}}{1+KC_{eq}} \quad (4)$$

$$q_{eq} = K_F C_{eq}^{n} \quad (5)$$

In the equations, q_{eq} is the load at equilibrium ($g_{adsorbate}/g_{adsorbent}$), q_{max} is the maximum number of available sites ($g_{adsorbate}/g_{adsorbent}$), C_{eq} is the concentration of adsorbate in the liquid at equilibrium (g/l), and the K, K_F and n are constants.[23]

Another common isotherm model is the BET (Brunauer-Emmet-Teller) model developed for gas phase adsorption. Equation 6 below has been reformulated for a liquid on solid adsorption.[34]

$$q_{eq} = q_{max} \frac{K_S C_{eq}}{(1-K_L C_{eq})(1-K_L C_{eq}+K_S C_{eq})} \quad (6)$$

Where K_S and K_L are equilibrium constants for the first layer of BET isotherms and upper layers respectively. The load at time t can be calculated from the following equations 7 and 8. Where $m_{adsorbate}$ is the mass of adsorbate adsorbed (g) at time t (s), Q is the flowrate (m^3/s), $C_{adsorbate}$ is the difference in concentration of the inlet and the outlet (g/l) and $m_{adsorbent}$ is the total mass of adsorbent in the column (g). [35]

$$m_{adsorbate} = Q \int_{t=0}^{t} C_{adsorbate}\, dt \quad (7)$$

$$q_t = \frac{m_{adsorbate}}{m_{adsorbent}} \quad (8)$$

The batch adsorption data from previous experiments using Organosorb 20-AA was reported by Sjölin et.al (2023)[36] to find the parameters of both Langmuir, Freundlich and BET isotherms. Since the data never reached a maximum concentration, the models were linearized, see Figure 4. The BET isotherm was best fitted to the data points of the impurities. However, the data points for HMF showed no trend. The large spread in data points for HMF made it difficult to estimate the parameters for a correct isotherm model.[36]

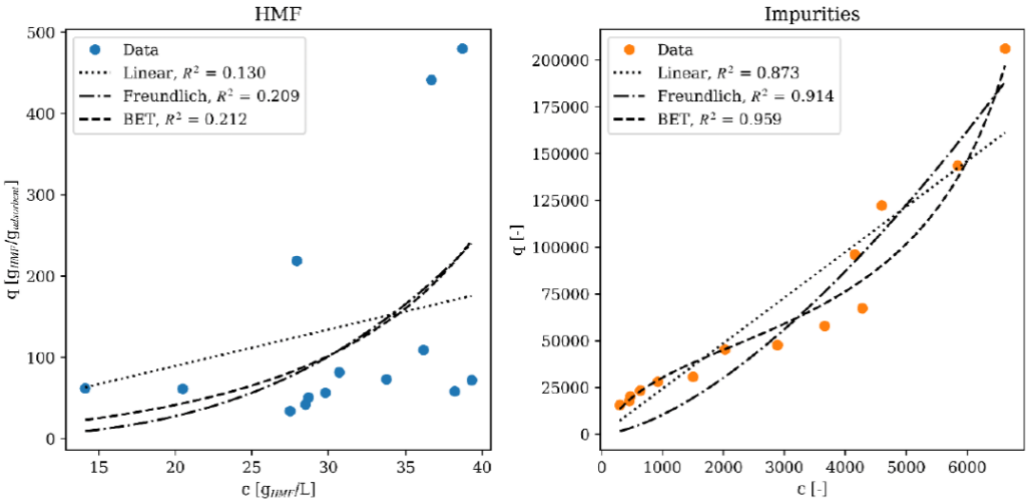

Figure 4. Data points form batch adsorption experiments, where the load, q, is plotted versus the concentration, c. Freundlich and BET isotherm models are fitted to the data points of HMF (left) and the impurities (right) respectively. Data by Sjölin et al. [36]

2.3.3. Kinetic Models

In order to describe the rate of adsorption, the kinetics of the process can be studied. There are in general four different steps that have effects on the rate of adsorption. The first step is molecule and/or ion transfer from the bulk to the boundary film of the liquid (bulk diffusion). The next step is transport from the boundary film to the surface of the adsorbent (film diffusion), followed by transport of ion from the surface to intraparticular active sites inside the porestructure (intraparticular diffusion). The last step is a chemical reaction via chelating, ion exchange or complexation. Depending on which step is the limiting in terms of adsorption rate, there are different types of models. The assumptions of the kinetic models are a constant temperature, a homogeneous bulk solution and that the mass transfer to, and in, the adsorbent can be described by diffusion.[13]

Two common models for describing kinetics are pseudo-first-order (PFO) and pseudo-second-order (PSO) models. Lagergren's rate equation is a pseudo-first-order model, see equation 9, describing adsorption from liquids. A pseudo-second-order equation is found in equation 10, where the occupancy rate to sites on the adsorbent is proportional to the square of the numbers of unoccupied sites.[23]

$$\frac{dq_t}{dt} = k_{kin}\left(q_{eq}(c) - q_t\right) \tag{9}$$

$$\frac{dq_t}{dt} = k_{kin}\left(q_{eq}(c) - q_t\right)^2 \tag{10}$$

In the equations, q_t is the load at time t ($g_{adsorbate}/g_{adsorbent}$), and q_{eq} is the load at equilibrium at concentration c ($g_{adsorbate}/g_{adsorbent}$). The terms k_{kin} are rate constants.[23]

There are several studies exploring the adsorption of HMF using activated carbon [18, 37, 38]. First order kinetics has been used as a model to describe the adsorption of HMF on GAC .The

side reactions to humins or other by-products are not researched enough, and it is believed that not all side reactions can be described by first-order kinetics.[18]

Sjölin.et.al. (2023)[36] observed that the adsorption of HMF was high in the beginning of the experiment, to then desorb when impurities started to adsorb on the GAC. Further the HMF adsorbed again later when the concentration of impurities had decreased in the bulk. This indicates that the impurities had a higher affinity to the surface than HMF. However, since HMF is smaller molecular than the impurities, it can diffuse into the pores of GAC faster and desorb when the impurities adsorb later, due to diffusion limitation from the surface to the available sites in the pores.[36] The large size of the humins might explain why the GAC with largest pore size was found to be the most efficient, since too narrow pores can sterically hindering and slow down the mass transfer.[25] It was also shown that the adsorption of humins can be well described by a pseudo-second-order model, but that the adsorption of HMF is harder to model due to the competitive adsorption. However, the pseudo-second-order model seems to be a better fit than the pseudo-first-order model for the HMF adsorption.[36]

2.3.4. Continuous Packed bed Adsorption of Humins

The continuous adsorption process investigated in this rapport has previously been simulated in Python by Sjölin.et.al (2023)[36], based on the previously presented batch experiments. The breakthrough curve is presented below, for an inlet concentration of 36 g/L of HMF and a porosity of 0.5. The column was 1 meter long, with a diameter of 0.1 meter. The feed was set to 36 g/L of HMF and 7500 integral adsorption units of humins. The simulation was based on the isotherm and adsorption kinetics of the batch experiments and used to estimate a reasonable residence time of 3.93 minutes. The simulation also shows that HMF can be collected for 54 minutes, before the outlet concentration of humins reach above 20 percent. However, the simulation was based on some assumptions and from previous batch experiment data. A breakthrough curve for the simulation is seen in Figure 5.[36]

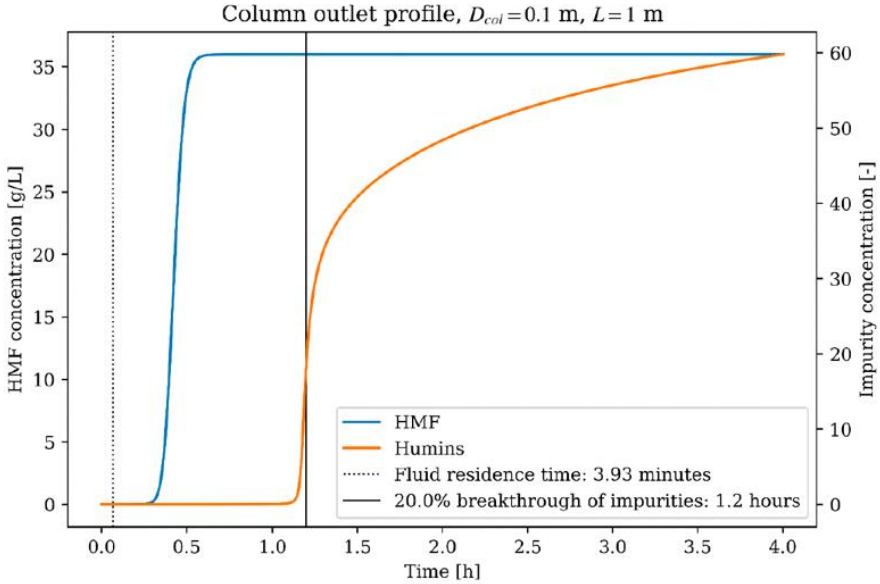

Figure 5. Simulated breakthrough curve for humins (impurities) and HMF, with a breakthrough at 20% humins by Sjölin et.al. (2023)[36].

2.3.5. Desorption

When the GAC packing becomes progressively saturated over time, the adsorption can no longer be performed. The GAC can then either be disposed or regenerated by desorption.[39] Several desorption techniques can be used to restore the capacity. On industrial scale, this is done continuously using redundancy columns that regenerate in parallel to the operating columns.[22]

Thermal desorption is the most common technique, using hot gases [40]. The thermal treatment generates 5-10 percent carbon losses that needs to be replaced with virgin carbon. If regeneration is required frequently, this will result in high costs. In addition, the process has a high energy demand since it requires temperatures. There are also in-situ regeneration techniques using chemical regeneration to desorb the molecules. The disadvantage of chemical regeneration is the use of additional chemicals. The eluent can also remain as residue that has a negative effect on the carbon.[32]

Since the optimal conditions of the batch experiments, mentioned before, still adsorbed roughly 20% of the HMF, desorption is valuable to retrieve the lost product from the separation. Sjölin et al. (2023)[36] investigated chemical desorption with water and DMC as elution media in different ratios for 48 hours. The results showed that HMF desorbed easier in DMC than in water. In addition, only a small amount of by-products was desorbed, indicating that the impurities are more strongly bound to the GAC than HMF. In contrast, more impurities desorbed using water.[36]

2.4. Analysis

To evaluate the results of the production of HMF and the adsorption, fructose conversion (%), HMF selectivity (%) and yield (%) was calculated, see equations 11-13 below.[22] The samples were analyzed by HPLC for HMF and fructose concentrations, and UV-VIS spectroscopy for humin concentration, described further in the next sections.

$$conversion = \frac{(fructose\ consumed\ in\ the\ reactor)}{(fructose\ feed\ to\ the\ reactor)} \quad (11)$$

$$selectivity = \frac{(HMF\ \ produced)}{(fructose\ consumed\ in\ the\ reactor)} \quad (12)$$

$$yield = \frac{(HMF\ produced)}{(fructose\ feed\ to\ the\ reactor)} \quad (13)$$

2.4.1. HPLC

High-performance liquid chromatography (HPLC) was used to analyze HMF and fructose concentrations. It is a common analytical method that uses high pressure to force a solvent through a packed column. The solvent, called the mobile phase, is mixed with the sample, and is then pumped through the packing, called the stationary phase. The different interactions for each compound in the mobile phase, with the stationary phase, will cause a separation over

time. The compounds have different retention times in the column, and the outflow is connected to a detector. The measurement of the detector gives a chromatogram, where the peaks can be used to estimate the amount of each compound. The interaction with the stationary phase is through hydrophobic, dipole-dipole or ionic bonds. The choice of solvent is therefore important since the polarity of the mobile phase effects the elution of the compounds.[41]

2.4.2. UV-Vis Spectroscopy

HPLC is not a suitable method for measurements of the humins, since the humins are a mix of compounds with different compositions, many unknown. For measurements of humins, spectroscopy can be used instead. Spectroscopy is based on analyzing chemical concentrations by using a passing beam of light through the sample. Compounds absorb light at different wavelengths, which is used in spectroscopy by shooting a light through one side of the sample while detecting what wavelengths go through to the other side. The results are shown in an absorption spectrum, a graph showing absorbance against wavelength. The concentration of a compound in the sample is directly proportional to the absorbance, which is described in Beer-lambert's law, equation 14, where A is the absorbance (-), ε is the molar absorptivity (l/(mol cm)), b is the pathlength (the width of the cell, cm) and c is the concentration (mol/l). If the sample absorbs too much light, it is hard to measure accurately since there is only a small amount of light passing through the sample. If the sample absorbs too little, the detector has a harder time distinguishing between the light passing through the sample and the reference.[41]

$$A = \varepsilon bc \tag{14}$$

The absorption spectrum for humins will not have a single peak since there are different compounds. By integrating the absorption spectrum and using Beer-Lambert's law, the total amount can be calculated. The method can in this case therefore only give relative numbers on reduction of humins compared to before the adsorption, not an exact number of the concentration.[41] Spectroscopy of humins have previously been studied by Sjölin (2023)[7] through UV-Vis spectroscopy, using all wavelengths in the visual spectrum (400-800 nm).

3. Method

This part describes the laboratory methods for the continuous dehydration of fructose and adsorption of humins. It also describes the procedures of the analysis methods HPLC (HMF and fructose) and UV-VIS spectroscopy. Lastly, the method for modelling the isotherm and kinetic models is presented.

3.1. Continuous Dehydration of Fructose

The method below was derived from previous experiments by Sayed et al. (2020) [16]. The experimental set-up is shown in Figure 6 below. First, the reactor was washed with a solution of 3:1 of DMC and water. The fructose solution was prepared by adding fructose powder in distilled water to a concentration of 300 gram per liter. The acidic catalyst, sulfuric acid or hydrochloric acid, was added to the desired pH. The organic solvent (DMC) was added into the fructose solution to the volume ratio 3:1 (organic:water phase). The solution was continuously stirred with a magnetic stirrer and pumped by an HPLC pump into a tubular coiled reactor with a volume of 18 ml. The tubular reactor was heated to 180-200 degrees Celsius with a silicon oil bath by using a hotplate while measuring the temperature with a thermocouple. It was assumed that the heat transfer from the oil to the reactor was efficient. After the reactor, a water bath was used to cool down the reaction medium to avoid formation of by-products. Different flow rates were tested to find the highest conversion and selectivity. The experiments were done by reacting 100 ml solution for each flow rate. Then the samples were analyzed in a HPLC, further described in 3.3, and the flow rate resulting in the highest selectivity of HMF and the highest fructose conversion was chosen to produce the targeted 1 liter of product. Finally, the phases were separated through a separation funnel, and the organic phase was filtered through a 100 µm filter cloth before being used in the adsorption experimental part. The samples were stored in a fridge at 4 °C before analysis and between the experimental steps to prevent further reactions.

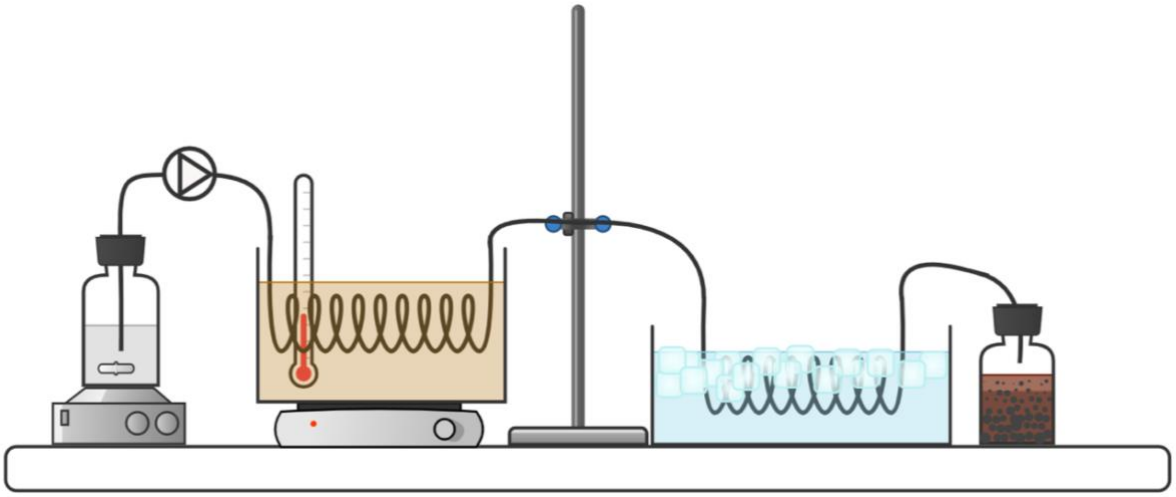

Figure 6. Sketch of the experimental set-up for the continuous dehydration.

3.2. Fixed Bed Adsorption

First the porosity of the GAC was determined by adding Organosorb 20-AA to a graduated cylinder to the 20 ml line. DMC was then added to the graduated cylinder, filling up the voids, and the mass of DMC added was weighted to calculate a volume of the void. The porosity was then determined according to equation 2. Before packing the column, the adsorbent was first washed with DMC to remove dust and then it was left over night in DMC to adapt prior to the experiments. The column was then packed, with a diameter and height of 20 mm. The temperature was controlled by pumping water into the jacket of the column, which was heated or chilled by a water bath. The dead volume of the system was measured by first filling the system with DMC, then pumping air and measuring the total volume DMC leaving the system.

Figure 7 shows a sketch of the experimental setup. The adsorption was initiated by first pumping pure DMC through the column, by a peristaltic pump, to prepare the column. The inlet of the flow is pumped from the bottom to the top of the column, to reduce the risk of air in the column. Then the inlet solution containing DMC, HMF and humins was fed, while mixed continuously. The mixing was done at a slow speed by a magnetic stirrer to decrease the risk of further reaction of HMF from the supplied mixing energy. The experiments were carried out at different temperatures (10-55°C) and residence times (4.2-15.6 min). The outlet of the column was pumped to a flask, while samples of 1.5 ml were collected in vials. The vials were stored in a fridge at 4 °C. The samples were used to measure HMF concentration through HPLC and amount of adsorbed humins by UV-VIS spectroscopy.

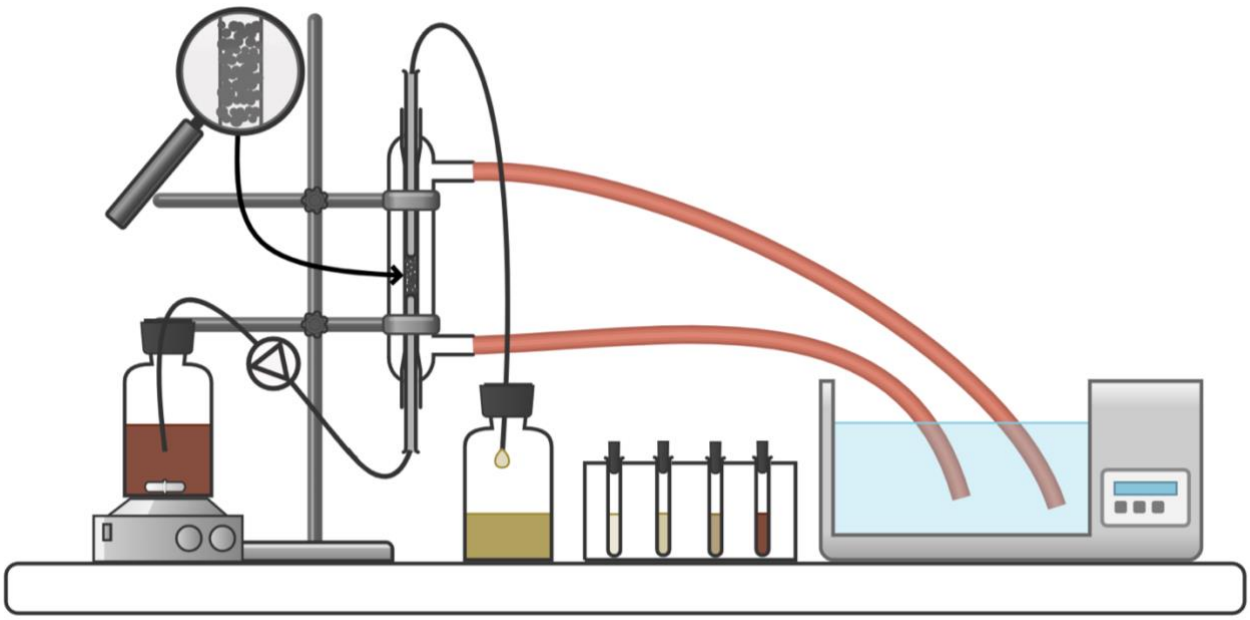

Figure 7. Sketch of the experimental set-up for the adsorption column.

3.3. Analytic Methods

For the analysis of fructose, HMF and humins, HPLC and UV-Vis spectroscopy was used.

3.3.1. HPLC

Prior to analysis, all samples were prepared by diluting 40 times in milli-Q water and syringe-filtered (0.2 μm) into vials.

The amount of unreacted fructose was measured after the dehydration reaction. The samples were analyzed in a Shimadzu HPLC system (Shimadzu Corporation, Kyoto, Japan), in a CarboSep CHO782 (Concise Separations, San Jose, CA, USA) column with deionized water as mobile phase. A RI detector was used, and the flowrate and temperature were 0.6 ml/min and 70 °C.

The concentration of HMF both after the dehydration reaction and throughout the adsorption was measured using a HPLC (JASCO, Tokyo, Japan) using a fast acid analysis HPLC column (Aminex HPX-87H column, Bio-Rad Laboratories, Hercules, CA, USA). The JASCO UV detector was operated at 254 nm and 0.5 mM sulfuric acid as the mobile phase. The temperature was set to 65 degrees with a flowrate of 0.2 ml/min.

3.3.2. UV-Vis Spectroscopy

The relative concentration of humins was measured by absorbance using a UV-1800 Shimadzu spectrophotometer 289 (Shimadzu Corporation, Kyoto, Japan). The samples were diluted with DMC and placed in quartz cells. Each sample was diluted to reach an absorbance between 0.5 and 1. The absorbances was measured over 400-800 nm wavelengths and the curve was then integrated to calculate the relative impurity reduction.

3.4. Modelling Adsorption Kinetics

To model the adsorption kinetics, a simulated model was fitted against the collected adsorption data using Python. The simulated model was received from Espinoza (2024)[42], and was based on dispersion, convection and an adsorption term, see equation 15 and 16, together with the different isotherm and kinetic models. The simulation also used the flowrate, F (m^3/h), porosity, ε, and dimensions of the packing with length and inner diameter, L (m) and d_i (m), matching the parameters used in the experiments.[42]

$$\frac{dc}{dt} = D_{ax}\frac{d^2c}{dx^2} - v\frac{dc}{dx} - \frac{dq}{dt}, \qquad 0 \leq x \leq L \tag{15}$$

$$\frac{dq}{dt} = f(c) \tag{16}$$

The time dependency of the concentration, c (g/l), of the adsorbed component is based on an axial dispersion term, with the dispersion coefficient D_{ax} (m^2/s), the convection based on the interstitial velocity, v_{int} (m/s), and the last term in equation 15 describing the load as a function of the concentration ($g_{adsorbate}/g_{adsorbent}$). The interstitial velocity (m/s) is obtained from equation

1, and the dispersion coefficient is calculated from the Peclet number, *Pe*, based on the Reynolds number, *Re*, using equations 17-19.[42]

$$Pe = v_{int} d_p D_{ax} \tag{17}$$

$$Pe = 12\varepsilon(0.2 + 0.011Re^{0.48}) \tag{18}$$

$$Re = v_{int}\rho\varepsilon d_p \eta \tag{19}$$

The particle diameter, *dp*, of the GAC was set to 1.5 mm, and the dynamic viscosity, η, and density, ρ, was set to those of pure DMC. Two Dirichlet boundary conditions were set, one for the inlet concentration, c_{in}, in the column and one of the concentration at the end of the column, see equations 20 and 21.[42] The initial values are set to 0 for the concentration, *c*, and the load, *q*,.[42]

$$\frac{dc}{dx} = c_{in}, \qquad x = 0 \tag{20}$$

$$\frac{dc}{dx} = 0, \qquad x = L \tag{21}$$

The model was then solved by the method of lines and discretizing by the finite volume method. The column was divided into 100 finite volumes. The second order derivatives were approximated using a three point central approximation, and for the first order a two point backward approximation was used. To solve the equations, `solve_ivp` from Python's SciPy library was used with the backward differentiation formula, BDF, method.[42] The model was fitted against the datapoints from the experiments using `curve_fit`, from the SciPy library, by varying the different constants in the isotherm and kinetic models.

To evaluate the fit of the kinetic models to the collected data in the adsorption xperiments, the coefficient R^2 from nonlinear least squares regression shown in equation 22 was used.[43] The *y* in the equation refers to the concentration.

$$R^2 = 1 - \frac{\sum_{k=1}^{n}(y_{k,data} - y_{k,model})^2}{\sum_{k=1}^{n}(y_{k,data} - \overline{y}_{k,model})^2} \tag{22}$$

4. Results & Discussion

The results and discussion section is divided into the three main parts: dehydration reaction experiments, adsorption experiments and future improvements.

4.1. Dehydration Reaction Experiments

The production of HMF through dehydration of fructose is presented in three parts. First, a tube reactor design to find an efficient reactor. Then different flow rates were evaluated, and based on the results the big batch was produced as a final part.

4.1.1. Tube Reactor Design

Four different continuous tube reactors were screened to produce HMF from fructose by a dehydration reaction. The characteristic of each reactor is listed in Table 1 below. The results for the experiments conducted of each reactor is presented in Appendix A.

Table 1. The design parameters for each reactor, including volume, inner & outer diameter and the heat transfer area based on the outer diameter.

Reactor	Material	Volume [ml]	Inner diameter [mm]	Outer diameter [mm]	Heat transfer area [cm^2]
1	1.4301 steel	2.4	1.5	3.0	128
2	1.4301 steel	8.2	3.0	6.0	219
3	1.4301 steel	4.2	2.0	4.0	168
4	1.4404 steel	18.0	3.0	6.0	480

The first reactor clogged on the first trial due to build up of humins, and no results are presented from this reactor. A larger diameter was therefore chosen for the second reactor, to decrease the risk of clogging, where different residence times, catalysts, and catalyst concentrations were evaluated. However, the results in Appendix A show that the conversion never reached above 42%. The reactor had a large diameter and a small heat transfer area, which resulted in an insufficient heat transfer. Therefore, the feed solution never reached the wanted temperature of 180 °C, which resulted in the low conversion.

Then a third reactor was constructed with a smaller diameter to increase the heat transfer from the oil bath to the feed inside of the reactor. However, the heating plate used could not heat the oil bath fast enough to keep a constant temperature throughout the experiments and the conversion was still not sufficient. The poor heating was due to an automatic temperature controller, which had disadvantageous PID control parameters that resulted in never reaching the set temperature. In addition, it was observed that the third reactor corroded in the last experiment, when green solution appeared in the outlet. Until then, mostly hydrochloric acid

had been used as a catalyst, which is known for its corrosive properties on metals due to its chloride ions [44].

For the experiments in the fourth and last reactor, only sulphuric acid was used as a catalyst to prevent corrosion. In addition, 1.4404 steel was used instead of 1.4301 steel to receive better corrosion resistance. The volume of reactor four was larger than the previous reactors which allowed a larger heat transfer area to achieve sufficient heat transfer and residence times. The heating plate was also exchanged to a manually controlled device, and the temperature of the oil bath could then be kept. Because of the increase in volume of the fourth reactor, the cooler was switched to one with the same dimensions as the reactor.

It was noticed that the reactor had a back pressure to the pump, even without any possible clogging of byproducts. This can be caused by evaporation of the reaction solvents d, which is not wanted for the dehydration. At such high temperatures, it is important that the pump can give enough pressure to keep the system in liquid phase. However, this could not be controlled, and it was assumed that the reaction medium was in liquid phase. The flowrate experiments using reactor 4 is presented in the next section.

4.1.2. Flowrate Experiments

For the continuous dehydration reaction of fructose to HMF, flowrates varied between 23 and 8 ml/min to find the best flowrate to produce the big batch. All experiments used sulfuric acid as catalyst with a pH of 1, and a temperature range between 180-200 °C. The temperature inside the reactor was assumed to be equal to the oil temperature, and that the temperature was constant throughout the whole reactor. The results of fructose conversion and HMF yield and selectivity is found with their flowrates and residence times in Table 2, with the experiments names A-H. The reason for doing a replicate of experiment G with experiment H was to test the reproducibility. A diagram presenting the experiments with the flowrates and the respective fructose conversion, HMF yield, and HMF selectivity is found in Figure 8. In the figure the results for flowrate 8 ml/min are presented as mean values from experiments G and H.

Table 2. Results of experiments A-H with their flowrate (ml/min), residence time (min), mean temperature of the oil bath (°C), fructose conversion (%), HMF yield (%) and HMF selectivity (%).

Experiment	Flowrate [ml/min]	Residence time [min]	Mean temperature [°C]	Fructose Conversion [%]	HMF Yield [%]	HMF Selectivity [%]
A	23.0	0.8	196	57.3	8.3	3.7
B	19.5	0.9	194	66.9	3.1	1.2
C	17.0	1.1	189	29.8	4.1	4.4
D	12.0	1.5	193	63.4	16.7	7.8

E	14.0	1.3	196	55.9	45.8	26.2
F	10.0	1.8	197	66.0	42.2	16.4
G	8.0	2.3	200	73.5	45.0	61.2
H	8.0	2.3	199	84.3	55.9	66.2

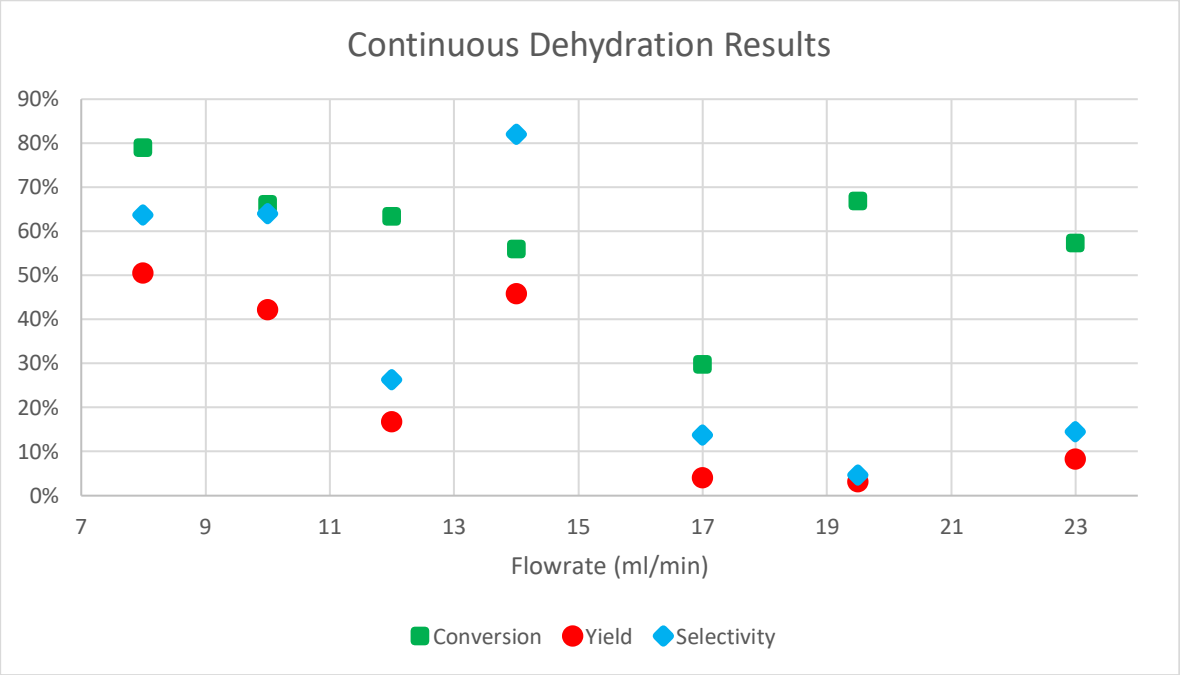

Figure 8. The results in fructose conversion (blue), HMF yield (orange) and HMF selectivity (yellow) for the different flowrates (ml/min).

There is a trend of higher conversion at longer residence times, seen in Figure 8, as expected from the background theory. However, both experiment A and B resulted in a high conversion, even if the residence times were short. Even at the high conversion, the selectivity and yield are very low. This means that the reaction did not form a significant amount of HMF, and the reaction has formed unwanted products instead. Figure 9 shows a visual representation of the 8 experiments. The color of experiment B is surprisingly light, typically this means that the fructose has not reacted, since both HMF and humins can visually be seen because of their colors. The high conversion in experiment B could be because of errors in the analysis, which can occur if the sample sent for analysis does not contain the water phase. Since fructose is only present in the water phase, a mixture of phases would result in a falsely high conversion.

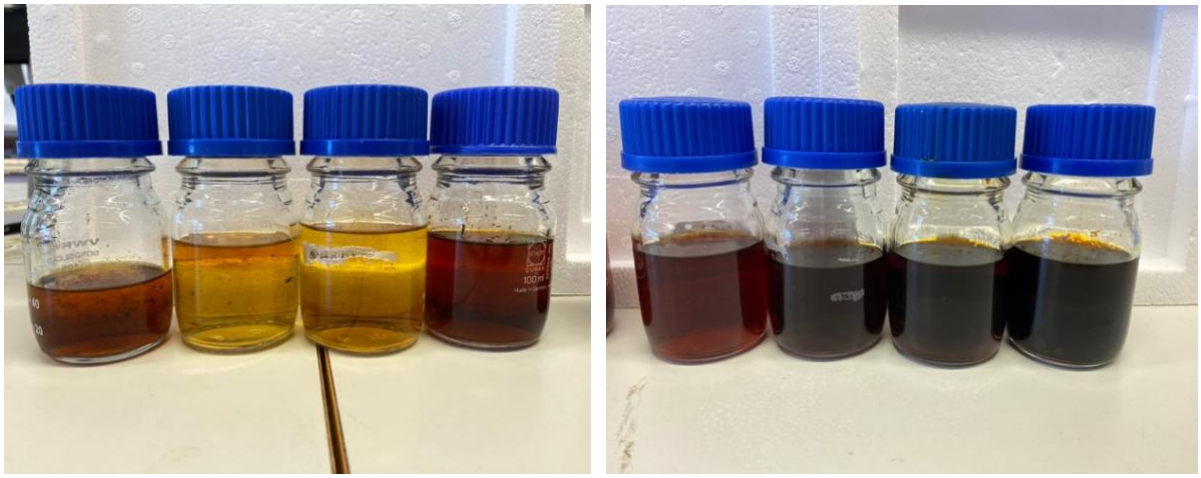

Figure 9. Shows the collected product stream for experiments A-H, from left to right.

The experiments were performed in the order A-G, which is an important note since there is a big risk that there has been build up during the experiments, which can impact the reactor volume and therefore also the residence time, and especially the heat transfer. It is observed in Figure 9 that experiment A produced large flakes of humins, that were unwanted in the adsorption part since it would build up in the tubes of the setup. The large flakes are correlated to the humins binding together, forming larger chains.

Experiment G and H both have the same experimental parameters. However, Table 2 shows a deviation in the results and that the experimental set-up was not able to reach a stable operating point. The non-stable setup makes it more complex to control the parameters, and there is a risk that the assumed parameters are not the real case. Assuming that the temperature inside the reactor is the same as the oil temperature, it could not be controlled easily by a thermometer since at such high temperatures, both DMC and water evaporates at atmospheric pressure. The temperature lower in the beginning of the reactor, increasing along the length. The temperature inside of the reactor is also not completely uniform. As the flowrate increases, the temperature assumption becomes less realistic. The heat transfer is also affected by the diameter and length of the column, as well as the choice of material. The buildup of humins on the inside of the reactor walls will also negatively affect the heat transfer, because of a thicker reactor wall, with a lower thermal conductive coefficient than steel.

The yield and selectivity increased at longer residence times. The best results were obtained at a flowrate of 8 ml/min, but it was still low compared to results from literature presented in the background. The average conversion, selectivity and yield was 78.9, 63.7 and 50.4 % for experiment G and H. However, to be able to move forward to the adsorption, the results were still considered satisfactory to give a reasonable representation of the HMF production process. An optimized reaction would have had a high conversion, with high yield and selectivity for HMF, reducing the amount of byproducts. This would result in a purer product stream, needing less purification and thus reducing the costs. For the adsorption part in this case, the byproducts can with advantage be used to see a significance in the purification step even at higher concentrations.

4.1.3. Big Batch

The big batch was produced with a flowrate of 8 ml/min based on the flowrate results. It was produced in two parts. The first part was produced in reactor 4, however after an hour of production the reactor clogged due to buildup of humins on the walls of the reactor. The flowrate experiments had an inlet volume of 100 ml and it was therefore not possible to predict to what extent that the reactor would clog when a larger volume was produced. When the production was interrupted, it was observed that the inlet solution seemed to only consist of one phase. This led to the conclusion that the stirring was insufficient and that the water phase with fructose sank to the bottom of the beaker due to density differences. As a result of this, the 3:1 ratio of DMC:water could not be kept constant, and an increased risk of byproduct formation was formed in the initial stages. This could also explain the color differences in the flow rate experiments, where a very dark initial color in the outlet was progressively becoming lighter during the experiments.

A new reactor, identical to reactor four, was used to produce the second part of the big batch. This time, a smaller beaker for the inlet solution was used to allow for more efficient stirring. However, this reactor also clogged only 15 minutes into the experiment even if the flowrate was increased to 10 ml/min, to reduce the risk of buildup of byproducts once again. The two parts produced 600 ml of organic phase in total, which was used for the adsorption experiments. The achieved conversion, yield and selectivity is found in Table 3 as well as the measured pH and absorbance of the organic phase after phase separation and filtration. The absorbance and HMF concentration were remeasured each time since it was observed that the absorbance varied, explaining the large deviation in the table below.

Table 3. Fructose conversion (%), HMF yield (%) and HMF selectivity (%) in the bigger batch of produced HMF, together with the measured absorbance and pH of the organic phase.

Humin absorbance [integral units]	**HMF conc [g/l]**	**pH [-]**	Fructose **Conversion [%]**	HMF **Yield [%]**	HMF **Selectivity [%]**
6496 ± 312	40.3 ± 0.83	1.5	82.7	42.9	51.8

4.2. Adsorption Experiments

The results of the adsorption experiments are presented in two sections, first the effect of residence time and then the temperature effect evaluation. The porosity of the GAC Organosorb 20-AA was determined to 0.6, according to equation 2. The dead volume of the set up was measured to 10.5 ml. With a diameter and height of 2 cm, the mass of Organosorb 20-AA was 2.9 g

4.2.1. Effect of Residence Time

First, three residence times were tested for the column at 25°C. The residence time was calculated from the flowrate according to equation 1, where the tortuosity was assumed to be 1, due to the large particle sizes. The break though curves are presented below in Figure 10-12 for experiment 1, 2 and 3 respectively.

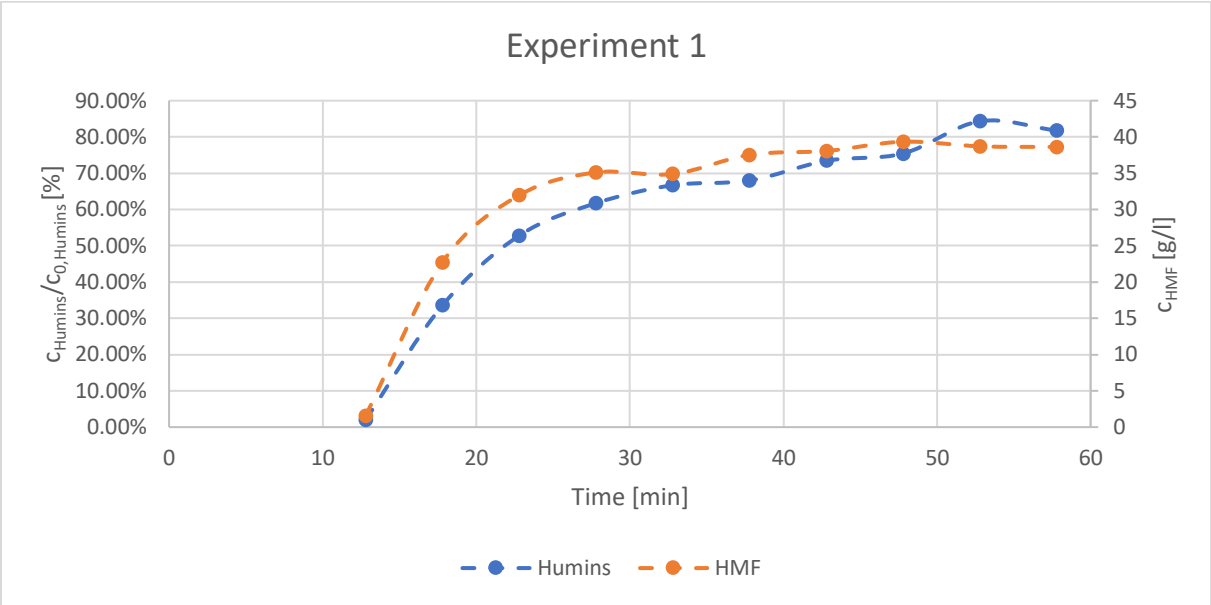

Figure 10. The break though curve for experiment 1 (25°C, 4.2 minute residence time). The data of HMF concentration (g/l) is shown in orange dots. The concentration of humins (%) is presented in concentration (-) divided by the inlet concentration(-), and is shown in the blue dots. Both concentrations are measured in the outlet of the column.

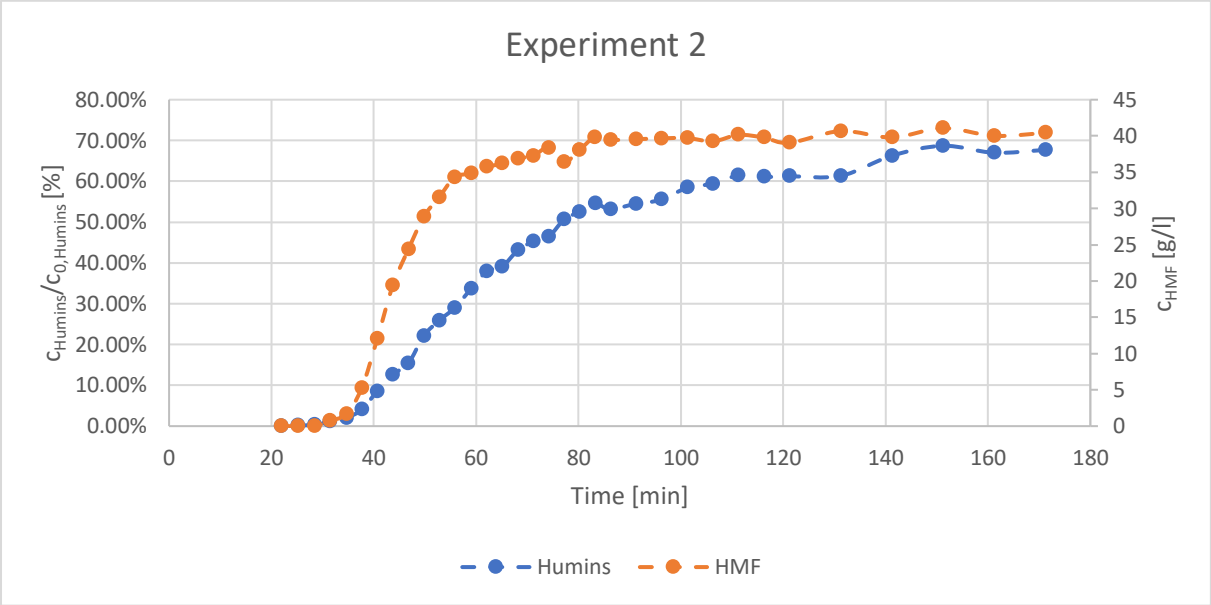

Figure 11. The break though curve for experiment 2 (25°C, 7.8 minute residence time). The data of HMF concentration (g/l) is shown in orange dots. The concentration of humins (%) is presented in concentration (-) divided by the inlet concentration(-), and is shown in the blue dots. Both concentrations are measured in the outlet of the column.

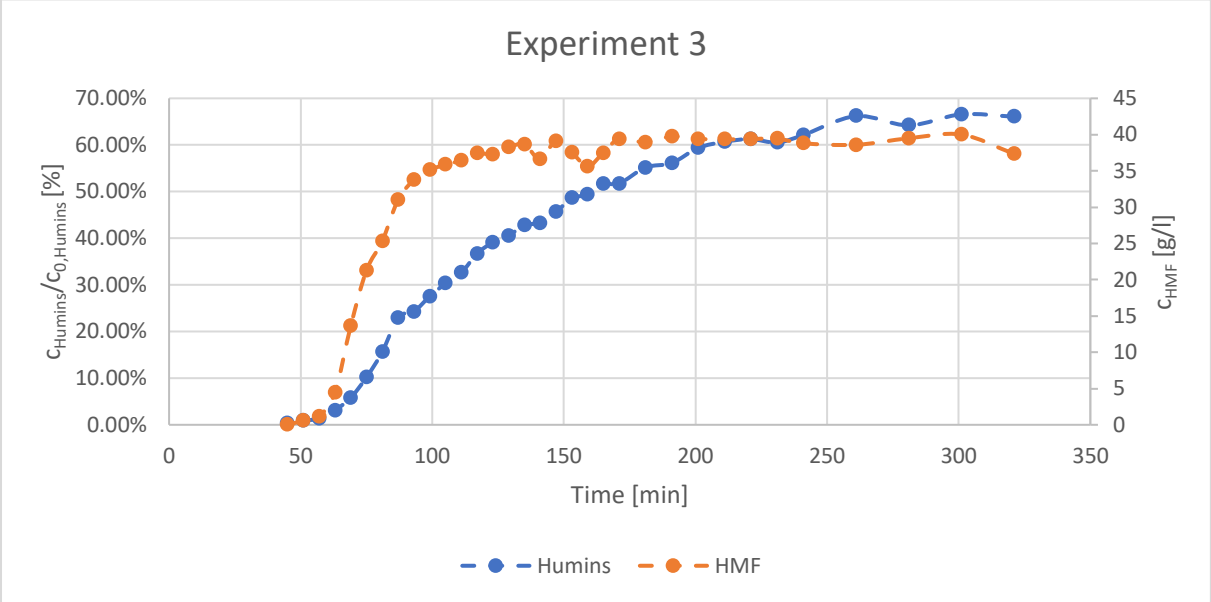

Figure 12. The break though curve for experiment 3 (25°C, 15.6 minute residence time). The data of HMF concentration (g/l) is shown in orange dots. The concentration of humins (%) is presented in concentration (-) divided by the inlet concentration (-), and is shown in the blue dots. Both concentrations are measured in the outlet of the column.

The results for the three experiments at 25°C are presented in Table 4. These results are based on that HMF can be collected until the concentration of humins in the outlet reaches a limit of 20% (C/C_0), based on the breakthrough presented in Figure 10-12. Experiments. 2 and 3 with 7.8- and 15.6-minutes residence time both resulted in a recovery of 0.1 gram of HMF before the outlet concentration of humins reached 20% (C/C_0). However, the concentration was slightly higher in experiment 3, and a residence of 15.6 minutes was therefore determined optimal since it would require less downstream processing removing the solvent. Experiment 3 also adsorbed the most amount of humins and had the lowest loss of HMF to the GAC, as seen in Table 4. Generally, the results show that the loss of HMF is decreasing when increasing the residence time. One could argue that a residence time of 7.8 minutes is the better choice in a scale-up, since the productivity is higher. The chosen residence time will be a tradeoff between productivity and the HMF purity prior to the downstream processing to remove the solvent.

The simulated adsorption column presented in section 2.3.4. had an optimal residence time of 3.93 minutes [36]. However, this residence time resulted in the lowest obtained amount of HMF in the experimental results. Even if experiment 1 had fewer measurement points, and thus less accuracy in the calculated results, the results still show a substantial difference in the concentration profiles compared to experiment 2 and 3. The column simulation was based on assumptions and used other parameter values, such as for the porosity and the inlet concentrations of both HMF and humins. It also used models for isotherms and kinetics based on batch experiments by Sjölin et al. (2023)[36].

Table 4. The results of the residence time experiments 1-3 at 25 °C at 20% breakthrough of humins.

Experiment	Residence time [min]	HMF Recovered [g]	HMF concentration outlet [g/l]	Humin concentration outlet [%]	HMF Loss [%]	Adsorbed humins [%]
1	4.2	0.02	4.3	6.6	89.7	93.8
2	7.8	0.10	7.9	5.3	81.0	94.7
3	15.6	0.10	10.1	5.6	74.8	94.4

4.2.2. Effect of Temperature

Figure 13 show the break though curve for experiment 4-6 at 15.6 minutes residence time at temperatures between 10-55 degrees Celsius. The results calculated for the four experiments is presented in Table 5.

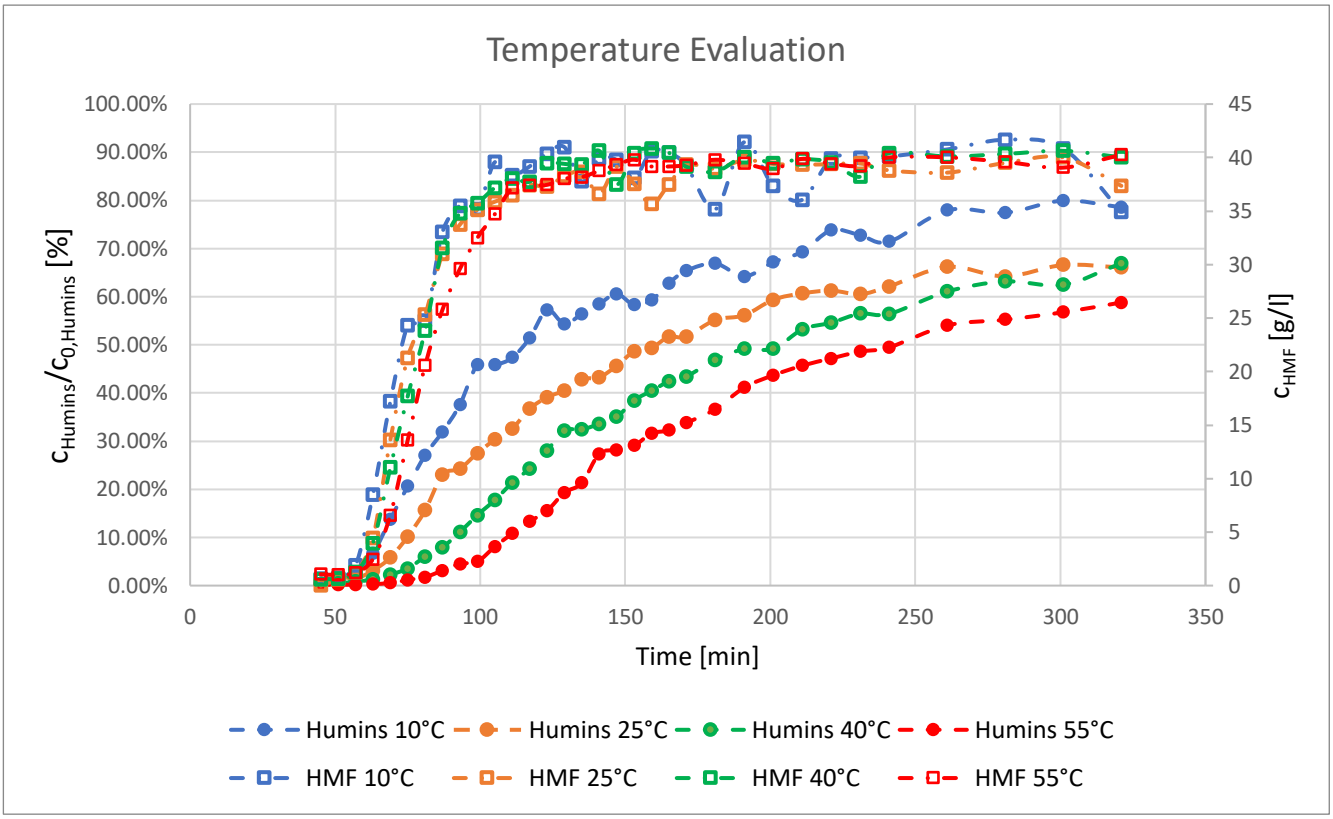

Figure 13. The break though curve for experiment 3-6 at 15.6 minutes residence time and a temperature of 10 (blue), 25 (orange), 40 (green) and 55 (red) degrees Celsius. The data of HMF concentration (g/l) is shown in squares. The concentration of humins (%) is presented in concentration (-) divided by the inlet concentration(-) and is shown in dots. Both concentrations are measured in the outlet of the column.

Table 5. The results of the experiments 3-6, varying the temperature between 10-55 °C at 15.6 minutes residence time at 20% breakthrough of humins.

Experiment	Temp [°C]	HMF Recovered [g]	HMF concentration outlet [g/l]	Humin concentration outlet [%]	HMF loss [%]	Adsorbed humins [%]
4	10	0.06	7.1	6.1	82.4	93.9
3	25	0.10	10.1	5.6	74.8	94.4
5	40	0.30	18.2	6.2	55.6	93.8
6	55	0.47	21.1	5.5	47.7	94.5

It can be concluded from the results in Table 4 and 5 that the temperature had a larger impact on the amount of recovered HMF than the residence time. The concentration profile for HMF did not change significantly with temperature, see Figure 13. However, it had an impact on the concentration profile for the impurities. As mentioned in the background, an increase in temperature results in faster diffusion to the surface of the GAC, but at the same time also higher desorption rates since the solubility increases and the potential for the components to bind decreases. The adsorption:desorption ratio for the humins increased at higher temperatures, indicating that the diffusion had a larger impact than the increase in solubility. This means that the outlet could be collected for a longer time at higher temperatures and recover more HMF, since it took longer for the impurity concentration to reach 20% of the inlet concentration. However, the adsorption cannot be performed at too high temperatures since it can cause the HMF to react further into more byproducts. The results are also in line with earlier studies mentioned, where the Organosorb 20-AA had the lowest BET surface, making diffusion limiting factor rather than the affinity to the surface. Further, there will be a maximum temperature where the HMF loss is at a minimum without further reaction to byproducts. Note that a higher temperature will result in a more energy demanding process and there will be a trade-off between energy consumption and HMF loss. However, since the fructose dehydration is at higher temperatures, the product stream can be cooled down to wanted adsorption temperature for efficient energy use.

Another important aspect is the limit of impurities that has been assumed 20% before breakthrough. If one can accept a lower quality product, the loss of HMF will be decreased. Although, the selling price will also decrease for lower degree of purity. However, the increased recovery of HMF at lower purity can be economically feasible even if the selling price decreases, depending on how the price changes with purity. It was found that HMF with a purity of 99% had more than dubbed the price compared to 95% purity [45].

The results have shown that continuous adsorption using GAC as an adsorbent is a suitable process for the purifying HMF, since all the experiments reached around 94 % removal of the impurities. However, there is still a loss of 48 % HMF in experiment 6. It would therefore be interesting to examine chemical desorption of the GAC to hopefully recover more HMF without desorbing the impurities. The loss of HMF is still too high for industrial profitability if the breakthrough is at 20% humins. Further, desorption of humins from GAC is also an important aspect for industrial scale-up, since regenerating the GAC reduces the material waste. Because of the difficulties to find a stable operating point in the production step, desorption experiments could not be performed due to time restriction.

4.3. Adsorption Kinetic Models

The data from experiment 6 was used to fit kinetic adsorption models. The data points were fitted to both pseudo first order (PFO) and pseudo second order (PSO) models, combined with the BET, Langmuir and Freundlich isotherm models shown in Figure 14-16 and Figure 17-19 for humins and HMF respectively. The estimated parameters are presented in Appendix B for each isotherm model for PFO and PSO respectively. The best fit was determined by the R^2 value as described in equation 24. It was assumed that there was no competitive adsorption since it was not observed in the concentration profiles.

The BET isotherm model obtained the highest R^2 for the humins, which can be seen in Figure 14-16. The PSO kinetic models also fitted the data set better for all isotherm models. The Freundlich isotherm model does not show a good correlation with the data. Visually, it can be observed that the BET isotherm fits better than the Langmuir isotherm at the last 4 data points for both PFO and PSO. Even if the R^2 for Langmuir is 0.99, the BET model seems to best describe the adsorption. This result further confirms the earlier simulations studied [42]. The Langmuir isotherm has a concentration profile that levels off, and based on Figure 14 there will be an overshoot of the model compared to the data. Since the goodness of fit is very similar for both kinetic models with the BET isotherm, it can be argued to use first order kinetics since it is a simpler model.

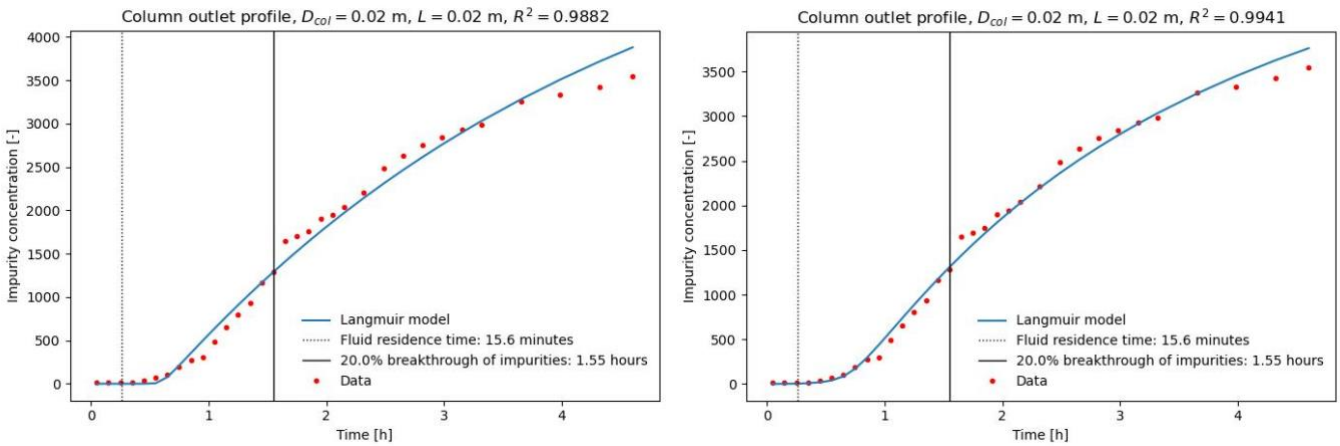

Figure 14. Humins adsorption kinetics fitted to dataset of experiment 6 using Langmuir isotherm (PFO left, PSO right)**.** The time axis does not include the dead volume.

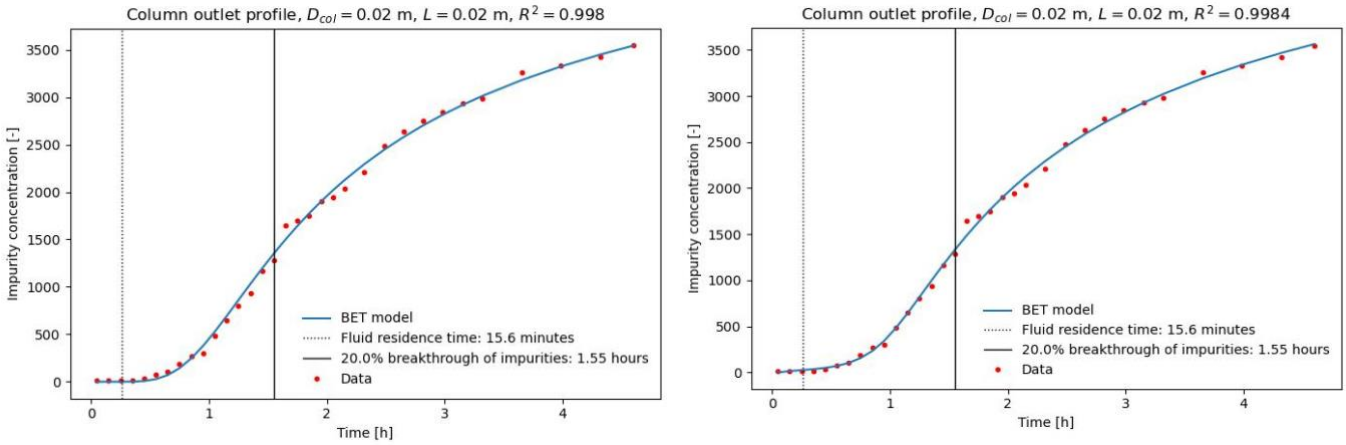

Figure 15. Humins adsorption kinetics fitted to dataset of experiment 6 using BET isotherm (PFO left, PSO right). The time axis does not include the dead volume.

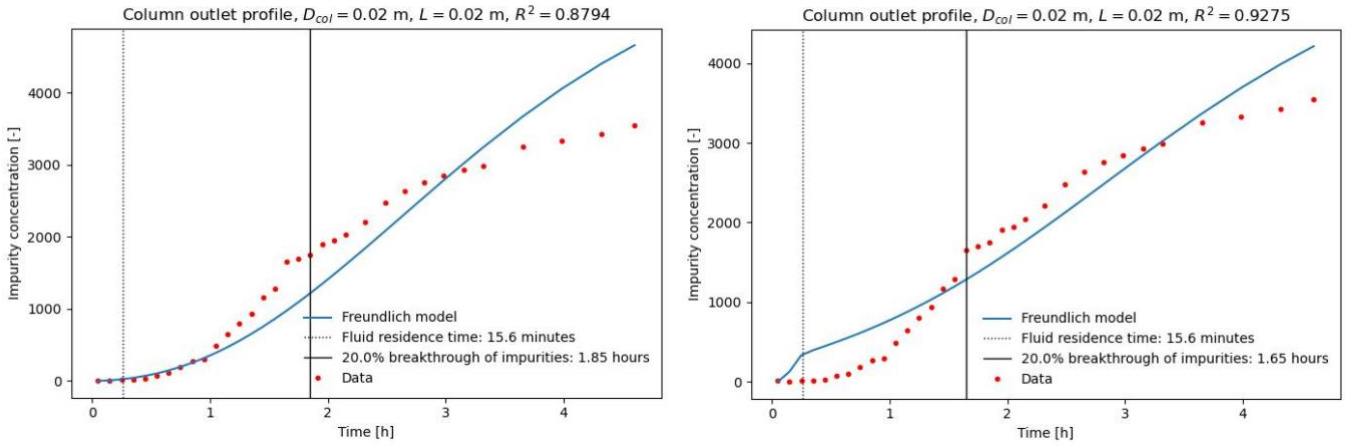

Figure 16. Humins adsorption kinetics fitted to dataset of experiment 6 using Freundlich isotherm (PFO left, PSO right). The time axis does not include the dead volume.

The corresponding graphs are plotted for HMF below in Figure 17-19. Here all graphs have a R^2 value >0.99 and it is therefore not clear which model fit the data set the best. Since the concentration profile for HMF levels off, compared to the data for humins, the Langmuir is in theory a good model. In addition, the Langmuir isotherm model together with a first order kinetic model is the simplest and was therefore preferred.

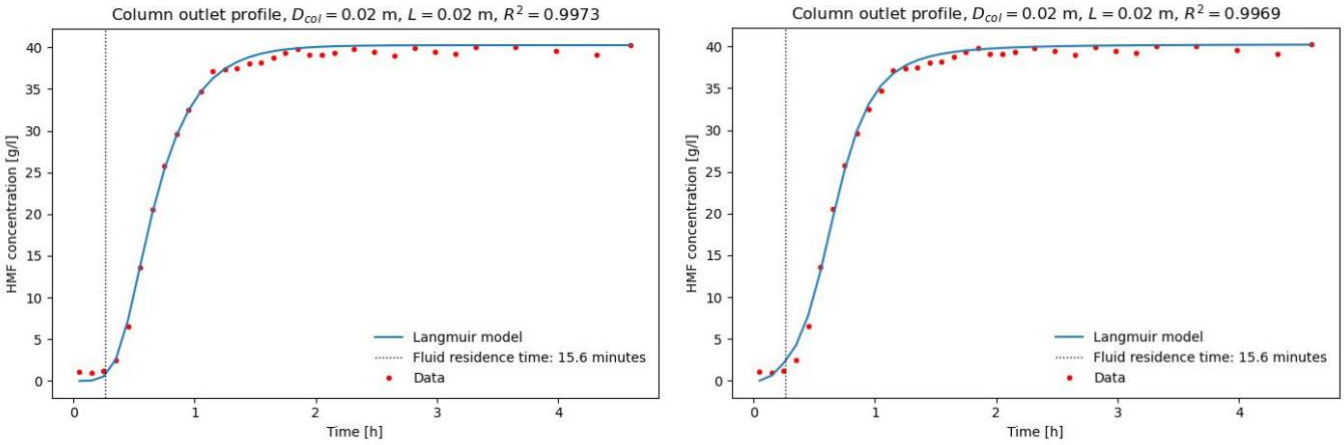

Figure 17. HMF adsorption kinetics fitted to dataset of experiment 6 using Langmuir isotherm (PFO left, PSO right). The time axis does not include the dead volume.

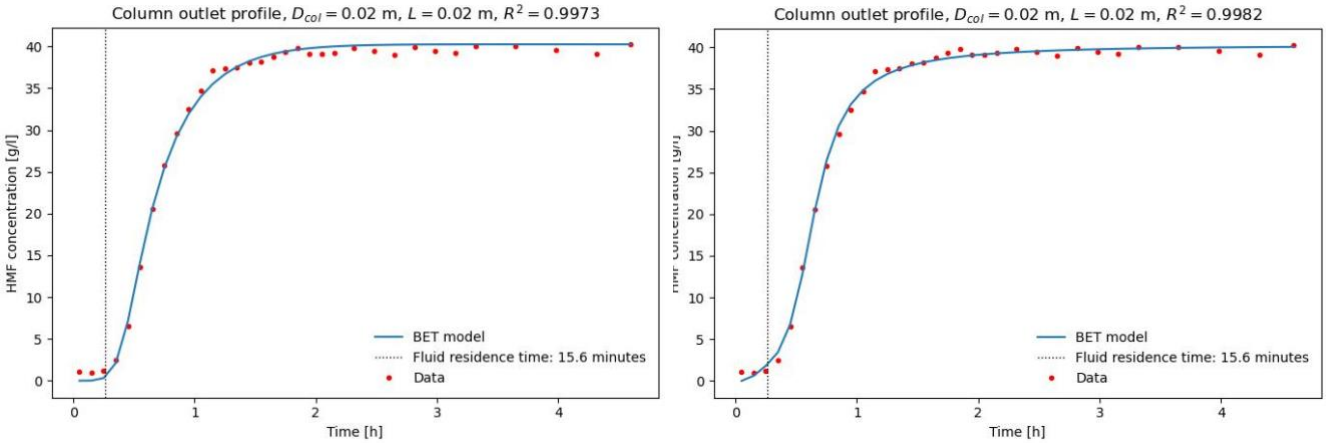

Figure 18. HMF adsorption kinetics fitted to dataset of experiment 6 using BET isotherm (PFO left, PSO right). The time axis does not include the dead volume.

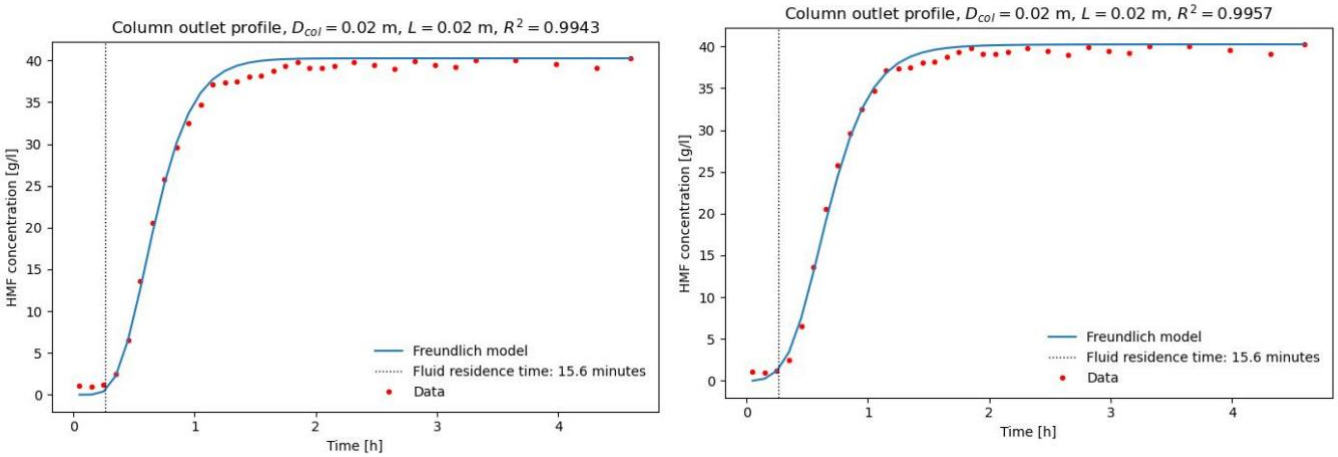

Figure 19. HMF adsorption kinetics fitted to dataset of experiment 6 using Freundlich isotherm (PFO left, PSO right). The time axis does not include the dead volume.

For the modelling part, it should be noted that the models are only fitted against one single dataset. This can lead to overfitted models, since the models have 3-4 parameters being varied. In theory, the parameters can be combined in more than one way to reach a model with a good fit. The risk of overfitting is increased in the BET isotherm model since it has 3 varying coefficients while the Langmuir and Freundlich only have 2. The most important result in this section is that it confirms that humin adsorption most likely follows the BET isotherm, and that the HMF adsorption follows an evident concentration profile, that appears to fit the Langmuir isotherm. By collecting more datasets at a given temperature, the models can be further calibrated and validated to get a more accurate model. The difference between the first and second order kinetics was insignificant and there is a higher risk of overfitting in the PSO model. This needs further evaluation to make a conclusion about the kinetic models.

4.4. Future Improvements

The most important improvement for the production of HMF is to find a stable operating point with reproducible results. The selected flowrate for the fructose dehydration reaction resulted in a lower conversion, selectivity, and yield than expected. More parameters such as temperature, pH, fructose concentration, and DMC:water phase ratio could be explored further to reach optimized results. As a result, less purification would be needed downstream in the process reducing the costs in large scale production.

The reactor clogged twice when producing the big batch and the volume produced was lower than planned. As a result, there was not enough organic phase to conduct more than one adsorption experiment at one temperature for isotherm model fitting. More datasets would give more accurate results in the kinetic and isotherm modelling for calibration and validation.

It was clear from the breakthrough curves that an increased temperature resulted in a more efficient separation, however a maximum temperature was never evaluated. Further the optimal results still show a loss of almost 50 % HMF, which could be recovered by chemical desorption of the GAC. As mentioned in the background, this has been investigated in batch and shows that HMF could be recovered by DMC, with some desorption of the impurities as well. This will be an important step in future scale-up. A reduction in the loss could also be achieved by optimization of more parameters in addition to residence time and temperature, including pH, different types of GAC, amount of adsorbent etc. Further, evaporation of DMC could be investigated for solvent regeneration. A techno economical analysis can be used to evaluate the trade-offs between energy demand and temperature, productivity and residence time, purities and selling prices as well as product loss and desorption.

5. Conclusion

The tube reactor design for the fructose dehydration concluded that a 1.4404 steel reactor with a heat transfer area of 480 cm^2 gave the most promising results at a temperature of 180-200 °C and a flowrate of 8 ml/min. The flowrate experiments showed that a residence time of 2.3 minutes resulted in the highest conversion, selectivity, and yield of 79, 64 and 50 % respectively. However, the production never reached a stable operating point, and the process needs further evaluation to allow for future scale-up.

The results of the continuous adsorption experiments showed that Organosorb 20-AA efficiently removed 95% of the impurities. The experiment at 16 minutes residence time and 55°C had the most efficient removal and resulted in a HMF concentration in the outlet at 21 g/l. However, the adsorption also resulted in a loss of 48% HMF. To decrease the loss, desorption of HMF using DMC is a promising method that should be appraised. Further, the trade-off between productivity, energy consumption, selling price and HMF loss needs to be considered.

The adsorption of humins is best described by the BET isotherm and pseudo first order kinetics. For HMF, the Langmuir isotherm pseudo together with pesudo first order kinetics shows a high potential of describing the adsorption. The modelling is only based on one dataset, and there is a risk of overfitting. Collecting more data is needed to further evaluate and confirm the models.

6. References

[1] P. Gabrielli *et al.*, "Net-zero emissions chemical industry in a world of limited resources," *One Earth,* vol. 6, no. 6, pp. 682-704, 2023/06/16/ 2023, doi: https://doi.org/10.1016/j.oneear.2023.05.006.

[2] A. Millot, A. Krook-Riekkola, and N. Maïzi, "Guiding the future energy transition to net-zero emissions: Lessons from exploring the differences between France and Sweden," *Energy Policy,* vol. 139, p. 111358, 2020/04/01/ 2020, doi: https://doi.org/10.1016/j.enpol.2020.111358.

[3] V. Haas, J. Wenger, L. Ranacher, N. Guigo, A. F. Sousa, and T. Stern, "Developing future visions for bio-plastics substituting PET – A backcasting approach," *Sustainable Production and Consumption,* vol. 31, pp. 370-383, 2022/05/01/ 2022, doi: https://doi.org/10.1016/j.spc.2022.02.019.

[4] E. Paone and F. Mauriello, "From bio-based furanics to biodegradable plastics," *Chem,* vol. 8, no. 4, pp. 897-899, 2022/04/14/ 2022, doi: https://doi.org/10.1016/j.chempr.2022.03.004.

[5] P. Stegmann, T. Gerritse, L. Shen, M. Londo, Á. Puente, and M. Junginger, "The global warming potential and the material utility of PET and bio-based PEF bottles over multiple recycling trips," *Journal of Cleaner Production,* vol. 395, p. 136426, 2023/04/01/ 2023, doi: https://doi.org/10.1016/j.jclepro.2023.136426.

[6] E. Weingart, S. Tschirner, L. Teevs, U. Prüße, M. Signoretto, and F. Menegazzo, "Conversion of Fructose to HMF in a Continuous Fixed Bed Reactor with Outstanding Selectivity," *Molecules,* Article vol. 23, no. 7, p. 1802, 2018, doi: 10.3390/molecules23071802.

[7] M. Sjölin, "Molasses Purification and Valorisation: Towards a sustainable production of hydroxymethylfurfural," Chemical Engineering, Lund University, 2023.

[8] S. Souzanchi, L. Nazari, K. T. V. Rao, Z. Yuan, Z. Tan, and C. Xu, "5-HMF production from industrial grade sugar syrups derived from corn and wood using niobium phosphate catalyst in a biphasic continuous-flow tubular reactor," *Catalysis Today,* vol. 407, pp. 274-280, 2023/01/01/ 2023, doi: https://doi.org/10.1016/j.cattod.2021.07.032.

[9] A. Mukherjee, M.-J. Dumont, and V. Raghavan, "Review: Sustainable production of hydroxymethylfurfural and levulinic acid: Challenges and opportunities," *Biomass and Bioenergy,* vol. 72, pp. 143-183, 2015/01/01/ 2015, doi: https://doi.org/10.1016/j.biombioe.2014.11.007.

[10] J. P. A. Silva, J. S. M. Nogueira, C. L. de Aquino Santos, and L. M. Carneiro, "9 - 5-Hydroxymethylfurfural as a chemical platform for a lignocellulosic biomass biorefinery," in *Production of Top 12 Biochemicals Selected by USDOE from Renewable Resources*, A. K. Chandel and F. Segato Eds.: Elsevier, 2022, pp. 269-315.

[11] F. Melo, R. Souza, P. Coutinho, and M. Oberson de Souza, "Synthesis of 5-Hydroxymethylfurfural from Dehydration of Fructose And Glucose Using Ionic Liquids," *Journal of the Brazilian Chemical Society,* vol. 25, 12/01 2014, doi: 10.5935/0103-5053.20140256.

[12] E. I. García-López, F. R. Pomilla, B. Megna, M. L. Testa, L. F. Liotta, and G. Marcì, "Catalytic Dehydration of Fructose to 5-Hydroxymethylfurfural in Aqueous Medium over Nb 2 O 5 -Based Catalysts," *Nanomaterials (2079-4991),* Article vol. 11, no. 7, pp. 1821-1821, 2021, doi: 10.3390/nano11071821.

[13] S. Liu *et al.*, "Advances in understanding the humins: Formation , prevention and application," *Applications in Energy and Combustion Science,* vol. 10, p. 100062, 2022/06/01/ 2022, doi: https://doi.org/10.1016/j.jaecs.2022.100062.

[14] Z. Cheng, J. L. Everhart, G. Tsilomelekis, V. Nikolakis, B. Saha, and D. G. Vlachos, "Structural analysis of humins formed in the Brønsted acid catalyzed dehydration of fructose," *Green Chemistry,* 10.1039/C7GC03054A vol. 20, no. 5, pp. 997-1006, 2018, doi: 10.1039/C7GC03054A.

[15] T. Okano, K. Qiao, Q. Bao, D. Tomida, H. Hagiwara, and C. Yokoyama, "Dehydration of fructose to 5-hydroxymethylfurfural (HMF) in an aqueous acetonitrile biphasic system in the presence of acidic ionic liquids," *Applied Catalysis A: General,* vol. 451, pp. 1-5, 2013/01/31/ 2013, doi: https://doi.org/10.1016/j.apcata.2012.11.004.

[16] M. Sayed *et al.*, "5-Hydroxymethylfurfural from fructose: an efficient continuous process in a water-dimethyl carbonate biphasic system with high yield product recovery," *Green Chemistry,* 10.1039/D0GC01422B vol. 22, no. 16, pp. 5402-5413, 2020, doi: 10.1039/D0GC01422B.

[17] S. Souzanchi, L. Nazari, K. T. Venkateswara Rao, Z. Yuan, Z. Tan, and C. Charles Xu, "Catalytic dehydration of glucose to 5-HMF using heterogeneous solid catalysts in a biphasic continuous-flow tubular reactor," *Journal of Industrial and Engineering Chemistry,* vol. 101, pp. 214-226, 2021/09/25/ 2021, doi: https://doi.org/10.1016/j.jiec.2021.06.010.

[18] T. D. Swift *et al.*, "Reactive adsorption for the selective dehydration of sugars to furans: Modeling and experiments," *AIChE Journal,* vol. 59, no. 9, pp. 3378-3390, 2013/09/01 2013, doi: https://doi.org/10.1002/aic.14090.

[19] Y. Xie, F. Yu, Y. Wang, X. He, S. Zhou, and H. Cui, "Salt effect on liquid–liquid equilibria of tetrahydrofuran/water/5-hydroxymethylfurfural systems," *Fluid Phase Equilibria,* vol. 493, pp. 137-143, 2019/08/01/ 2019, doi: https://doi.org/10.1016/j.fluid.2019.04.018.

[20] W. Guo, Z. Zhang, J. Hacking, H. J. Heeres, and J. Yue, "Selective fructose dehydration to 5-hydroxymethylfurfural from a fructose-glucose mixture over a sulfuric acid catalyst in a biphasic system: Experimental study and kinetic modelling," *Chemical Engineering Journal,* vol. 409, p. 128182, 2021/04/01/ 2021, doi: https://doi.org/10.1016/j.cej.2020.128182.

[21] J. Esteban, A. J. Vorholt, and W. Leitner, "An overview of the biphasic dehydration of sugars to 5-hydroxymethylfurfural and furfural: a rational selection of solvents using COSMO-RS and selection guides," *Green Chemistry,* 10.1039/C9GC04208C vol. 22, no. 7, pp. 2097-2128, 2020, doi: 10.1039/C9GC04208C.

[22] S. Robin, *Chemical Process Design and Integration*, 2nd ed ed. Chichester, West Sussex, United Kingdom: Wiley (in English), 2016.

[23] P. Pourhakkak, A. Taghizadeh, M. Taghizadeh, M. Ghaedi, and S. Haghdoust, "Chapter 1 - Fundamentals of adsorption technology," in *Interface Science and Technology*, vol. 33, M. Ghaedi Ed.: Elsevier, 2021, pp. 1-70.

[24] Z. Aksu and F. Gönen, "Biosorption of phenol by immobilized activated sludge in a continuous packed bed: prediction of breakthrough curves," *Process Biochemistry,* vol. 39, no. 5, pp. 599-613, 2004/01/30/ 2004, doi: https://doi.org/10.1016/S0032-9592(03)00132-8.

[25] M. Alveteg, Ed. *Separationsprocesser*. Lund University: Department of Chemical Engineering, 2019.

[26] F. Wesenauer, C. Jordan, M. Azam, M. Harasek, and F. Winter, "Considerations on Temperature Dependent Effective Diffusion and Permeability of Natural Clays," *Materials (1996-1944),* Article vol. 14, no. 17, p. 4942, 2021, doi: 10.3390/ma14174942.

[27] F. E. Bartell, T. L. Thomas, and Y. Fu, "Thermodynamics of Adsorption from Solutions. IV. Temperature Dependence of Adsorption," *The Journal of Physical Chemistry,* vol. 55, pp. 1456-1462, 1951.
[28] G. Newcombe, "Chapter 8 - Removal of natural organic material and algal metabolites using activated carbon," in *Interface Science and Technology*, vol. 10, G. Newcombe and D. Dixon Eds.: Elsevier, 2006, pp. 133-153.
[29] C. Ng, W. Marshall, R. Rao, R. Bansode, J. Losso, and R. Portier, "Granular Activated Carbons from Agricultural By-products: Process Description and Estimated Cost of Production," 08/01 2003.
[30] K. S. W. Sing, "Adsorption methods for the characterization of porous materials," *Advances in Colloid and Interface Science,* vol. 76-77, pp. 3-11, 1998/07/01/ 1998, doi: https://doi.org/10.1016/S0001-8686(98)00038-4.
[31] K. R. Crincoli, P. K. Jones, and S. G. Huling, "Fenton-driven oxidation of contaminant-spent granular activated carbon (GAC): GAC selection and implications," *Science of The Total Environment,* vol. 734, p. 139435, 2020/09/10/ 2020, doi: https://doi.org/10.1016/j.scitotenv.2020.139435.
[32] A. Larasati, G. D. Fowler, and N. J. D. Graham, "Insights into chemical regeneration of activated carbon for water treatment," *Journal of Environmental Chemical Engineering,* vol. 9, no. 4, p. 105555, 2021/08/01/ 2021, doi: https://doi.org/10.1016/j.jece.2021.105555.
[33] R. R. Gonzales, Y. Hong, S. H. Kim, J. H. Park, and G. Kumar, "Kinetics and equilibria of 5-hydroxymethylfurfural (5-HMF) sequestration from algal hydrolyzate using granular activated carbon," (in English), *Journal of Chemical Technology and Biotechnology,* Article vol. 91, no. 4, pp. 1157-1163-1163, 04/01/ 2016, doi: 10.1002/jctb.4701.
[34] A. Ebadi, J. S. S. Mohammadzadeh, and A. Khudiev, "What is the correct form of BET isotherm for modeling liquid phase adsorption?," (in English), *Adsorption,* Journal Article vol. 15, no. 1, pp. 65-73, 02/01/ 2009, doi: 10.1007/s10450-009-9151-3.
[35] J. Lo´pez-Cervantes, D. I. Sa´nchez-Machado, R. G. Sa´nchez-Duarte, and M. A. Correa-Murrieta, "Study of a fixed-bed column in the adsorption of an azo dye from an aqueous medium using a chitosan-glutaraldehyde biosorbent," (in English), *Adsorption Science & Technology,* Journal Article vol. 36, no. 1-2, pp. 215-232, 02/01/ 2018, doi: 10.1177/0263617416688021.
[36] M. Sjölin, M. Sayed, D. Espinoza, S. Tallvod, and B. Al-Rudainy, "Regeneration of dimethyl carbonate and purification of 5-hydroxymethylfurfural used in a biphasic dehydration process through activated carbon adsorption and evaporation," Manuscript, 2023.
[37] N. Rajabbeigi, R. Ranjan, and M. Tsapatsis, "Selective adsorption of HMF on porous carbons from fructose/DMSO mixtures," *Microporous and Mesoporous Materials,* vol. 158, pp. 253-256, 2012/08/01/ 2012, doi: https://doi.org/10.1016/j.micromeso.2012.03.047.
[38] W. C. Yoo, N. Rajabbeigi, E. E. Mallon, M. Tsapatsis, and M. A. Snyder, "Elucidating structure–properties relations for the design of highly selective carbon-based HMF sorbents," *Microporous and Mesoporous Materials,* vol. 184, pp. 72-82, 2014/01/15/ 2014, doi: https://doi.org/10.1016/j.micromeso.2013.10.001.
[39] P. Márquez, A. Benítez, A. F. Chica, M. A. Martín, and A. Caballero, "Evaluating the thermal regeneration process of massively generated granular activated carbons for

their reuse in wastewater treatments plants," *Journal of Cleaner Production,* vol. 366, p. 132685, 2022/09/15/ 2022, doi: https://doi.org/10.1016/j.jclepro.2022.132685.
[40] A. Larasati, G. D. Fowler, and N. J. D. Graham, "Chemical regeneration of granular activated carbon: preliminary evaluation of alternative regenerant solutionsElectronic supplementary information (ESI) available. See DOI: 10.1039/d0ew00328j," *Environmental Science: Water Research & Technology,* vol. 6, no. 8, pp. 2043-2056, 01/01/Number 8/2020 2020, doi: 10.1039/d0ew00328j.
[41] D. C. Harris and C. A. Lucy, *Quantitative chemical analysis*, Tenth edition ed. Macmillan International Higher Education, 2020.
[42] D. Espinoza, "Model simulation in pyhton, script," ed, 2024.
[43] S. Nakagawa and H. Schielzeth, "A general and simple method for obtaining R2 from generalized linear mixed-effects models," *Methods in Ecology and Evolution,* vol. 4, no. 2, pp. 133-142, 2013/02/01 2013, doi: https://doi.org/10.1111/j.2041-210x.2012.00261.x.
[44] R. Fan, W. Zhang, Y. Wang, D. Chen, and Y. Zhang, "Metal Material Resistant to Hydrochloric Acid Corrosion," *Journal of Physics: Conference Series,* vol. 1732, no. 1, p. 012134, 2021/01/01 2021, doi: 10.1088/1742-6596/1732/1/012134.
[45] "5-hydroxymethylfurfural." MOLBASE. https://www.molbase.com/cas/67-47-0-storeType-0-purity-99%25-sellUnit-0-leadTime-on-countryId-0-grade-0-vip-0-storeLevel-0-minPrice-0-maxPrice-0-p-1.html (accessed 17.05, 2024).

Appendix

Appendix A

The parameters for the second and third reactor are presented in Table A1 and A3 respectively and results for the two reactors are presented in Table A2 and A4 below. No results are presented for the first reactor since it clogged on the first trail. Some experiments resulted in a negative conversion and selectivity, due to poor accuracy in the experimental measurements. These results should be seen as 0 % conversion. Further, at low conversions the selectivity is in some cases above 100%, a result of bad accuracy. These should be seen as 100%.

Table A1. The parameters used in experiments 1-8 for the second reactor. The pH was measured in the water phase and added catalyst percentage refers to volume percentage of the water phase.

Experiment	Flowrate [ml/min]	Residence time [min]	pH [-]	Added catalyst [%]	Mean temperature [°C]	Catalyst
1	10.0	0.8	1.5	-	177	H_2SO_4
2	8.2	0.9	1.2	-	172	HCl
3	8.2	1.1	1.3	-	180	H_2SO_4
4	7,0	1.3	0.1	-	181	HCl
5	6.0	1.5	1.0	-	177	HCl
6	5.5	1.8	-	1	178	HCl
7	7.0	2.3	-	2	178	HCl
8	5.0	2.3	-	2	181	HCl

Table A2. The results for conversion (%), yield (%) and selectivity (%) for experiments 1-8 in the second reactor.

Experiment	Conversion [%]	Yield [%]	Selectivity [%]
1	-3.4	1.1	-32.5
2	1.2	1.9	154.9
3	41.7	2.8	6.8
4	8.3	1.8	21.4
5	2.9	1.6	54.1
6	41.1	2.5	6.0
7	1.8	3.7	211.1
8	12.6	4.5	35.9

Table A3. The parameters used in experiments 9-14 for the third reactor. The pH was measured in the water phase and added catalyst percentage refers to volume percentage of the water phase.

Experiment	Flowrate [ml/min]	Residence time [min]	pH [-]	Added catalyst [%]	Mean temperature [°C]	Catalyst
9	4.0	1.05	-	2	181	HCl
10	6.1	0.69	-	2	176	HCl
11	7.1	0.60	-	2	182	HCl
12	6.5	0.65	-	2	185	HCl
13	6.5	0.65	0.7	-	176	H_2SO_4
14	7.0	0.60	0.7	-	184	H_2SO_4

Table A4. The results for conversion (%), yield (%) and selectivity (%) for experiments 9-14 in the second reactor.

Experiment	Conversion [%]	Yield [%]	Selectivity [%]
9	38.0	6.0	15.1
10	92.7	38.1	41.1
11	20.9	6.1	29.1
12	-4.1	6.4	-154.2
13	26.5	9.3	34.9
14	70.4	17.8	25.3

Appendix B

The BET, Langmuir and Freundlich isotherm parameters used to simulate PSO and PFO kinetic model for humins and HMF are presented below in Table B1-B3. The R^2 value describes how well the kinetic model fitted the set of datapoints from the adsorption result of experiment 6.

Table B1. The modelled BET isotherm parameters for HMF and humins modelled for pseudo first and second order kinetic models.

Parameter	HMF (PFO)	HMF (PSO)	Humins (PFO)	Humins (PSO)
q_{max} [$g_{adsorbate}/g_{adsorbent}$]	9810	14500	20700	20500
K_S [$(g/L)^{-1}$]	$4.14 \cdot 10^{-3}$	$8.48 \cdot 10^{-4}$	$2.38 \cdot 10^{-4}$	$4.89 \cdot 10^{-3}$
K_L [$(g/L)^{-1}$]	-0.0853	-0.0338	$1.62 \cdot 10^{-4}$	$1.59 \cdot 10^{-4}$
K_{kin} [PSO: 1/min] [PFO:($g_{adsrobent}$/($g_{adsorbate}$ min))]	$1.14 \cdot 10^{-6}$	$3.49 \cdot 10^{-8}$	$2.89 \cdot 10^{-5}$	$4.79 \cdot 10^{-11}$
R^2 [-]	0.9973	0.9982	0.9980	0.9984

Table B2: The modelled Freundlich isotherm parameters for HMF and humins with pseudo first and pseudo second order kinetic models.

Parameter	HMF (PFO)	HMF (PSO)	Humins (PFO)	Humins (PSO)
K_F [$(g_{adsorbate}/g_{adsorbent}) \cdot (L/g)^n$]	1.85	1.08	2.43	8.17
n [-]	1.00	1.15	1.19	1.07
K_{kin} [PSO: 1/min] [PFO:($g_{adsrobent}$/($g_{adsorbate}$ min))]	$3.00 \cdot 10^{-5}$	$1.34 \cdot 10^{-5}$	$3.85 \cdot 10^{-6}$	$5.80 \cdot 10^{-11}$
R^2 [-]	0.9943	0.9957	0.8794	0.9275

Table B3: The modelled Langmuir isotherm parameters for HMF and humins with pseudo first and pseudo second order kinetic models.

Parameter	HMF (PFO)	HMF (PSO)	Humins (PFO)	Humins (PSO
$\mathbf{q_{max}}$ [$g_{adsorbate}/g_{adsorbent}$]	88.6	186	104000	161000
K [(g/l)-1]	0.175	0.0178	0.183	0.0344
$\mathbf{K_{kin}}$ [PSO: 1/min] [PFO:($g_{adsrobent}$/($g_{adsorbate}$ min))]	$2.31 \cdot 10^{-6}$	$3.11 \cdot 10^{-7}$	$1.55 \cdot 10^{-7}$	$6.76 \cdot 10^{-13}$
$\mathbf{R^2}$ [-]	0.9973	0.9969	0.9882	0.9941